Mon. Not. R. Astron. Soc. **000**, 1–?? (2005) Printed 5 February 2008 (MN LATEX style file v2.2)

A complete N-body model of the old open cluster M67

Jarrod R. Hurley[1,2⋆], Onno R. Pols[3], Sverre J. Aarseth[4] and Christopher A. Tout[4]
[1] *Centre for Stellar and Planetary Astrophysics, School of Mathematical Sciences, Monash University, VIC 3800, Australia*
[2] *Department of Astrophysics, American Museum of Natural History, Central Park West at 79th Street, New York, NY 10024, USA*
[3] *Astronomical Institute, Utrecht University, Postbus 80000, 3508 TA Utrecht, the Netherlands*
[4] *Institute of Astronomy, Madingley Road, Cambridge CB3 0HA, UK*

Accepted 2005 Month xx. Received 2005 Month xx; in original form 2005 May 26

ABSTRACT
The old open cluster M67 is an ideal testbed for current cluster evolution models because of its dynamically evolved structure and rich stellar populations that show clear signs of interaction between stellar, binary and cluster evolution. Here we present the first truly direct N-body model for M67, evolved from zero age to 4 Gyr taking full account of cluster dynamics as well as stellar and binary evolution. Our preferred model starts with 36 000 stars (12 000 single stars and 12 000 binaries) and a total mass of nearly $19\,000 M_{\odot}$, placed in a Galactic tidal field at 8.0 kpc from the Galactic Centre. Our choices for the initial conditions and for the primordial binary population are explained in detail. At 4 Gyr, the age of M67, the total mass has reduced to $2\,000 M_{\odot}$ as a result of mass loss and stellar escapes. The mass and half-mass radius of luminous stars in the cluster are a good match to observations although the model is more centrally concentrated than observations indicate. The stellar mass and luminosity functions are significantly flattened by preferential escape of low-mass stars. We find that M67 is dynamically old enough that information about the initial mass function is lost, both from the current luminosity function and from the current mass fraction in white dwarfs.

The model contains 20 blue stragglers at 4 Gyr which is slightly less than the 28 observed in M67. Nine are in binaries. The blue stragglers were formed by a variety of means and we find formation paths for the whole variety observed in M67. Both the primordial binary population and the dynamical cluster environment play an essential role in shaping the population. A substantial population of short-period primordial binaries (with periods less than a few days) is needed to explain the observed number of blue stragglers in M67. The evolution and properties of two thirds of the blue stragglers, including all found in binaries, have been altered by cluster dynamics and nearly half would not have formed at all outside the cluster environment. On the other hand, the cluster environment is also instrumental in destroying potential BSs from the primordial binary population, so that the total number is in fact slightly smaller than what would be expected from evolving the same binary stars in isolation.

Key words: stellar dynamics—methods: N-body simulations— stars: evolution— blue stragglers– binaries: close— open clusters and associations: general

1 INTRODUCTION

Star clusters have long been recognized as important tools for understanding many astrophysical processes. As such they are the focus of many observational programs, both from the ground (e.g. Kalirai et al. 2003; Kafka et al. 2004) and space (e.g. Grindlay et al. 2001; Piotto et al. 2002; Richer et al. 2004). Dynamical modelling had its beginnings over four decades ago (von Hoerner 1960; Aarseth 1966; van Albada 1968) but it is only recently that the models have reached a state where genuine comparison with cluster observations is possible. This is the result of software advances that have improved realism and speed as well as a huge increase in hardware performance. The realm of globular clusters is still out of reach of realistic direct N-body models. So it is open clusters that garner initial attention in the attempt to confront cluster models with observations and vice-versa. In particular, old open clusters are of interest because these are dynamically well-evolved and offer the chance to observe the effects of interaction between stellar, binary and cluster

⋆ E-mail: jarrod.hurley@sci.monash.edu.au (JRH)

evolution. A good example is M67 which contains an abnormally large number of blue straggler (BS) stars for its age and size (Ahumada & Lapasset 1995), as well as a good proportion of X-ray sources (van den Berg et al. 2004). Both are indicators that the cluster environment has affected the evolution of the stars. M67 is also close enough to be well studied and within range of current N-body modelling capabilities[1]. The idea is that by matching the characteristics of a model cluster and the observed cluster we can learn about the initial conditions, binary population and dynamical evolution of the cluster. In doing this we must bear in mind the need to marry theoretical and observational data reduction techniques (Portegies Zwart et al. 2004).

The interest in M67 and its BSs stems not only from the large number of BSs but also from their diverse nature. Observations indicate that 60 per cent are in spectroscopic binaries (Milone & Latham 1992; Latham & Milone 1996). Of those in binaries the orbits are a mixture of short-period and eccentric, long-period and eccentric, and long-period and circular. Blue stragglers are identified in a cluster colour-magnitude diagram (CMD) by their position above and blueward of the main-sequence turn-off. A popular explanation for their existence is that they are rejuvenated main-sequence (MS) stars that have gained hydrogen-rich material. Mass transfer in a binary from a companion to a MS star is an obvious means by which this can occur. There are three main scenarios (Kippenhahn, Wiegert & Hoffmeister 1967) distinguished by the stellar type of the mass donor, MS star (Case A), sub-giant or red giant (Case B), or asymptotic giant branch (AGB) star (Case C). Case A mass transfer can produce a BS in a very short-period Algol system, but in many cases ends in coalescence of the two MS stars when angular momentum is lost from the system and the orbit shrinks. This produces single BSs. Case B mass-transfer occurs in slightly wider binaries and results in a short-period circular binary containing a BS with a white dwarf companion. BSs in longer period binaries may be produced by Case C mass transfer or by accretion of material from an AGB star wind. The binary orbit will be circular except in some cases of wind accretion. However current models of binary tides and wind accretion only allow for accretion to occur and the orbit to retain an eccentricity in binaries with periods in excess of a few thousand days and the degree of accretion drops for wider orbits. This is a known problem in attempts to explain the existence of Barium stars in eccentric binaries (Pols et al. 2003). Thus binary evolution alone fails to explain the full range of BSs found in M67 and, in particular, the short-period eccentric binaries. It also fails to explain the so-called super-BS observed in M67 (Leonard 1996) which has a mass greater than twice that of the cluster MS turn-off mass, $M_{\rm TO}$. Blue stragglers could also form as a result of direct collisions between MS stars although this is unlikely as the timescale for such an event to occur in an open cluster is too long (Press & Teukolsky 1977; Mardling & Aarseth 2001).

[1] M67 has been identified by the MODEST collaboration (Sills et al. 2003) as an ideal cluster for various groups working on cluster evolution models to compare simulation techniques and use the observed data to calibrate the models: see `http://manybody.org/modest/projects.html`.

In Hurley et al. (2001) we presented a semi-direct N-body model of M67. We showed that the combination of the cluster environment and a large population of binaries is able to generate formation paths for all of the BSs observed in M67. BSs were found in wide eccentric binaries because the BSs were exchanged into such orbits in three- and four-body encounters subsequent to their formation. Cases where two MS stars forming the inner binary of a triple system merged and remained bound to the third star were also observed and these produced BSs in short-period eccentric orbits. Roughly half of the BSs formed during the simulation were the result of standard binary evolution in primordial binaries. The remainder owed their existence in some way to dynamical encounters. Some were the result of perturbations to primordial binaries. The orbits of these binaries are dynamically altered so that mass-transfer begins whereas the stars would have remained detached if evolved in isolation. Collisions between MS stars at periastron in highly eccentric binaries also proved to be an efficient BS formation pathway. These eccentric binaries were the result of exchange interactions or perturbations to the orbits of primordial binaries. Super-BSs were also formed after the merger of three or more MS stars – an example of this sees a single BS formed via Case A mass transfer and then exchanged into an eccentric binary where it collides with its new MS companion. So this simulation was successful in showing that the cluster environment is able to boost BS production and that the diverse nature of the M67 BSs can be explained if they formed by a variety of mechanisms. However, the model did not generate enough BSs in binaries at any single moment – at most 25% of the BSs were in binaries when the model was at or near the age of M67.

The main failing of the Hurley et al. (2001) M67 model was that it is semi-direct. By this we mean that, owing to computational constraints, the model was not evolved by the direct N-body method for its entirety. At the time special-purpose hardware for computing gravitational forces was available in the form of the GRAPE-4 (Makino & Taiji 1998) and while this had given a substantial increase in the performance of N-body codes it still did not allow a complete model of M67 to be evolved from birth in a timely manner. The complication that M67 has a high frequency of binaries further reduced the simulation rate. The method employed by Hurley et al. (2001) was to take a population of 5 000 single stars and 5 000 binaries and evolve these from birth to an age of 2.5 Gyr according to a rapid stellar and binary evolution algorithm (Hurley, Tout & Pols 2002) – standard population synthesis. This evolved population was then used as input to the N-body code and evolved further to the age of M67 (about 4 Gyr, see next section). The results of previous N-body simulations were used as a guide when selecting the stars and binaries for the model and to generate the density profile for the starting N-body model. So every effort was made to account for the effect of processes such as mass-segregation during the 2.5 Gyr of cluster evolution that was skipped. However the situation was far from ideal. Since that time N-body capabilities have improved markedly with the arrival of the next generation of special-purpose hardware, the GRAPE-6 (Makino et al. 2003), and its teraflops speed. In the meantime there have also been software and host-CPU speed-ups to aid with binaries (see Aarseth 2003). As a result binary-rich open clusters are now within reach

of direct N-body codes (Hurley & Shara 2003) as are larger single-star models (Baumgardt & Makino 2003). So we can now perform a direct model of M67.

In this paper we attempt to create a direct N-body model of the old open cluster M67. We discuss the model in comparison with observations of M67, looking at the overall structural properties and the nature of the stellar populations. In Section 2 we describe the parameters of our starting model and in Section 3 we look at the nature of the primordial binary population in some detail. We describe our simulation method in Section 4. Section 5 contains the results of our first attempt at a model of M67 and then in Section 6 we present our favoured M67 model. This is followed by a discussion and summary of our results in Section 7.

2 THE INITIAL MODEL

The goal is to evolve an N-body model cluster from zero-age to obtain a model that resembles M67 at its current age in terms of both structural parameters and stellar populations. Unfortunately we cannot observe M67 at zero-age so in setting up our initial model we must be guided by observations of M67 at present in combination with the behaviour of previous cluster models and also observations of young open clusters. In this section we discuss in turn our choices for the metallicity and age of M67, the binary fraction, the stellar initial mass function, the initial mass of the cluster, the tidal field and the density profile. The details of the primordial binary population are left for Section 3. We consider two models (blandly called Model 1 and Model 2) which differ only in the initial mass and the tidal field, and in the period distribution of the primordial binaries. All other choices are the same for both models.

It is generally accepted that M67 stars are of solar composition (Hobbs & Thorburn 1991; Tautvaišienė et al. 2000). There is no reason to believe that the metallicity of M67 has varied over its life so we take $Z = 0.02$ for our initial model. The age of M67 is less settled with values quoted in the literature ranging from 3.2 ± 0.4 Gyr (Bonatto & Bica 2003) to as high as 6.0 Gyr (Janes & Phelps 1994). In Hurley et al. (2001) we assumed an age of 4.2 Gyr based on fitting the isochrones of Pols et al. (1998) to the available data. Recently VandenBerg & Stetson (2004) derived an age of 4.0 Gyr for M67. We shall investigate behaviour around 4 Gyr in the current study while bearing in mind that the cluster may be slightly younger or older.

M67 is definitely a binary-rich cluster. Montgomery, Marschall & Janes (1993) found that at least 38 per cent of the cluster stars are binaries based on analysis of the photometric binary sequence in the colour-magnitude diagram (CMD). A high binary frequency was confirmed by Fan et al. (1996) and Richer et al. (1998) who both found 50 per cent to be consistent with their data. How this translates to a primordial binary fraction depends somewhat on the parameters of the primordial binaries and the evolution of the cluster. A good indicator is to look at the evolution of binary fraction in previous open cluster models. Shara & Hurley (2002) performed simulations starting with 18 000 single stars and 2 000 binaries – a primordial binary fraction of 0.1. The orbital separations of the binaries were drawn from the distribution suggested by Eggleton, Fitchett & Tout (1989) with a peak at 30 au and limits of 0.03 au (about $6R_\odot$) and 30 000 au. This distribution was based on the Bright Star Catalogue (Hoffleit 1983) and is in agreement with the period distribution found by Duquennoy & Mayor (1991). After 4.5 Gyr of cluster evolution, Shara & Hurley (2002) found that the binary fraction was still close to 0.1. The evolution of binary fraction is shown in Figure 1 for one of their models. Also shown is the binary fraction for a simulation presented by Hurley & Shara (2003) which began with 12 000 single stars and 8 000 binaries. They used the same distribution for the initial orbital separations but set the maximum at 200 au. This means the 40 per cent binaries would actually represent a population of 55 per cent binaries if the upper limit were set at 30 000 au. In both cases the binary fraction remains similar as the cluster evolves. This can be understood because, while encounters may destroy soft binaries and a combination of dynamical hardening and binary evolution may destroy very hard binaries, the preferential escape of low-mass single stars from the cluster via tidal stripping counteracts these effects on the binary fraction. With a high fraction of primordial binaries residing in the high density core we do expect many binaries to be lost in binary-binary encounters. However, even in this region of the cluster the binary fraction does not drop because single stars are ejected from the core in the same encounters (Aarseth 1996). The conclusion is that, for reasonable choices of the binary parameters, experience shows that in open cluster simulations the primordial binary fraction is well preserved as the cluster evolves. Therefore we assume a primordial binary fraction of 0.5 and elaborate on the particulars of these binaries in the next section.

Single star initial masses are chosen from the initial mass function (IMF) of Kroupa, Tout & Gilmore (1993, KTG93) between the mass limits of 0.1 and $50M_\odot$. All stars are assumed to be on the zero-age main sequence (ZAMS) when the simulation begins. This means that we neglect any age spread in the cluster stars that may be caused by differences in the pre-main sequence evolution timescales or by more than one epoch of star formation. We also assume that any residual gas from the star formation process has been removed.

The number of stars in the initial model, or alternatively the initial mass of the cluster M_0, is an important quantity. To estimate it is difficult for us because determination of the current mass of M67 from observations suffers from incompleteness and converting this to an initial mass requires knowledge of the mass-loss history from the cluster. A lower limit of approximately $800M_\odot$ for the current mass of M67 was set by Montgomery et al. (1993). Later Fan et al. (1996) established that M67 has about $1\,000M_\odot$ in nuclear-burning stars with masses greater than $0.5M_\odot$. We shall refer to this as the luminous mass, $M_{\rm L}$. Hurley et al. (2001) showed that this corresponds to a total cluster mass, M, of $2\,500M_\odot$ and $M_0 \simeq 3\,500M_\odot$ if stellar and binary evolution are taken into account but the influence of the dynamical cluster environment is ignored. However, stars in a cluster are subject to mass segregation and this process, combined with the stripping of stars by the tidal field of the Galaxy, alters the mass function of the cluster over time to give a deficiency of low-mass stars. Looking at previous N-body data available to us (Shara & Hurley 2002; Hurley & Shara 2003) we find that $M_{\rm L} = 1\,000M_\odot$ is more likely to represent

a total mass of approximately $1\,400 M_\odot$ after 4 Gyr of stellar, binary and cluster evolution. We note that the limiting radius of the Fan et al. (1996) observations was 10 pc while the tidal radius of M67 is greater and therefore the actual mass of the cluster may be slightly higher.

Next we must convert the current mass to an initial mass. Hurley et al. (2001) estimated that a starting model of 40 000 stars would be required to make a full model of M67. This was based on models with an escape rate parameter $k_{\rm e} = 0.3$ (see their equation 18). They also took the initial half-mass radius to be 1 pc which gave a starting model well within its tidal radius. N-body models starting with 30 000 stars and no primordial binaries have recently been presented by Hurley et al. (2004). Analysis of these models shows that $k_{\rm e} = 0.3$ is once again suitable to describe the average escape rate over the lifetime of the cluster. Using this value, and taking $M_0 = 15\,000 M_\odot$ for a cluster that fills its tidal radius initially and has a half-mass radius, $r_{\rm h}$, of 5 pc (giving a half-mass relaxation timescale of about 300 Myr), we find that approximately $2\,000 M_\odot$ in stars is left after 4 Gyr. This neglects mass loss owing to stellar evolution and there is also a degree of redundancy in the analysis but it shows that something of this order is required for the starting model. The 30 000 single-star models of Hurley et al. (2004) actually had $M \approx 5\,800 M_\odot$ at 4 Gyr which is too high for M67. However, it has been shown (Hurley & Shara 2003) that the presence of a large number of primordial binaries increases the escape rate of stars and this is confirmed in our future paper on the general trends of binary-rich open cluster evolution (Hurley et al., in preparation). We note that the escape rate analysis of Hurley et al. (2001) does not consider the effect of binaries. Based on all this we start in our first attempt (Model 1) with 9 000 single stars and 9 000 binaries which gives $M_0 \simeq 14\,400 M_\odot$, comparable to that of the 30 000 single-star models.

In Model 1 we assume for simplicity that the cluster is subject to a standard Galactic tidal field for the Solar neighborhood, a circular orbit with a speed of $220\,{\rm km\,s^{-1}}$ at a distance of 8.5 kpc from the Galactic centre. For a mass of $14\,400 M_\odot$ this gives a tidal radius, $r_{\rm t}$, of 34 pc. M67 actually has a slightly eccentric orbit with a perigalacticon of 6.8 kpc and an apogalacticon of 9.1 kpc (Carraro & Chiosi 1994). We will therefore consider a second model (Model 2) starting with 12 000 single stars and 12 000 binaries on an orbit at 8.0 kpc from the Galactic centre but leave further details of this to Section 6, after we have presented the results for the first model.

The density profile chosen for our starting model is that of a Plummer model (Plummer 1911; Aarseth, Hénon & Wielen 1974). There is no reason to believe that a King model (King 1966), the major alternative, should describe the initial state of an open cluster as this set of models was originally conceived to describe dynamically evolved globular clusters. Kroupa, Aarseth & Hurley (2001) built a model of the Orion Nebula cluster which for simplicity used a Plummer density profile. They also assumed that the model contained twice the mass in gas as it had in stars and then after 0.6 Myr of N-body evolution the gas was removed smoothly. The result was not only a bound cluster but, after 100 Myr, the projected radial density profile was a good fit to that of the Pleiades. In fact the choice is not likely to be crucial because previous N-body studies (e.g. Hurley & Shara 2003) have shown that an initial Plummer model quickly evolves to resemble a King profile. The density profile in combination with the assumption that the stars are in virial equilibrium generates the initial positions and isotropic velocities of the stars. Formally the Plummer model extends to infinite radius so in the rare case of large distance (more than $10 r_{\rm h}$) a rejection is applied. The length-scale parameter is chosen such that the cluster fills its tidal radius from the beginning of the simulation. The position of the outermost star lies at a distance of 34 pc from the cluster centre. The choices for both starting models are summarized in Table 1.

3 PARAMETERS OF THE PRIMORDIAL BINARY POPULATION

When setting up a population of primordial binaries we must choose how to distribute their orbital parameters. For each binary we need an orbital separation, a (or period, P), an eccentricity, e, and masses for the two stars (or one mass, which may be the total binary mass, $M_{\rm b}$, and a mass ratio, q). The distribution function chosen for the orbital separation or period is generally guided by observations with popular choices being a flat distribution of $\log a$ (Abt 1983) or a log-normal distribution (Eggleton, Fitchett & Tout 1989; Duquennoy & Mayor 1991). For the eccentricity a choice is usually made between a thermal distribution (Heggie 1975), $f(e) = 2e$, or simply to have all orbits initially circular (although $e = 0.0$ is generally avoided for numerical reasons). When determining the masses of the component stars these may be uncorrelated, each mass is drawn independently from the same IMF, or a distribution of mass ratios may be assumed.

In view of the relatively large number of blue stragglers found in M67, Hurley et al. (2001) performed a binary population synthesis study to determine which combination of distribution functions for the orbital parameters of the primordial binaries would maximize the number of blue stragglers produced. Binaries were evolved according to the binary star evolution (BSE, Hurley, Tout & Pols 2002) code. They found that choosing the orbital separation from a flat distribution of $\log a$ in combination with correlated masses could possibly reproduce the M67 BS number provided that all BS producing binaries are retained by the cluster over its lifetime. So in this case standard evolution of primordial binaries is enough without the dynamical interactions between cluster stars. However, the nature of the synthetic BS population does not correspond with that of the observed population. Only 25 per cent of the BSs are in binaries and all of these have circular orbits with almost all having an orbital period of less than a year. Therefore, even if the cluster environment does not have a role to play in creating BS formation channels, it must be affecting the evolution of the binaries and the nature of the BS population.

The case of uncorrelated component masses was ruled out by Hurley et al. (2001) because it leads to too few BSs by far. Their favoured population synthesis model had the Eggleton, Fitchett & Tout (1989) separation distribution with a peak at 10 au and a maximum of 200 au in combination with correlated masses and a thermal eccentricity distribution. The 200 au limit was based on the realisation that binaries wider than this would be weakly bound and

broken-up by dynamical encounters. This model predicted that about ten of the M67 BSs could be produced from standard binary evolution of primordial binaries with 30% of the BSs in binaries, all with circular orbits. Hurley et al. (2001) then evolved their semi-direct model with the primordial binaries set up in this way. When the model reached an age of 4.2 Gyr there were 22 BSs present. Unfortunately only one of the BSs present at 4.2 Gyr was still in a binary.

A problem with the Hurley et al. (2001) semi-direct M67 model was that no BSs were found in wide circular binaries at any time during the evolution while two are currently observed in M67 (Latham & Milone 1996). Exchange interactions do not tend to produce binaries in circular orbits so it would seem that the evolution of primordial binaries must produce any BSs in wide circular binaries. This can occur as a result of stable Case C mass transfer from an AGB star or via wind accretion. On inspection of the binary population in their starting model in combination with the setup of the BSE algorithm used to evolve the binaries, Hurley et al. (2001) discovered that no such binaries were expected. They found that if they repeated the binary population synthesis with the wind velocity reduced by a factor of two[2] and the weaker criterion of Webbink (1988) used to detect the onset of dynamical mass transfer (as opposed to the default for the BSE algorithm) that the number of BSs predicted at 4.2 Gyr rose by 25 per cent for their favoured choice of distribution functions. More important the mix of the BS population was 22 per cent in wide circular binaries (up from 0 per cent), 22 per cent in close circular binaries (down from 28 per cent) and 56 per cent single (down from 72 per cent). We use a period of 1 000 d to make the distinction between close and wide binaries. In this paper we have used $\beta = 1/8$ and the Webbink (1988) test for dynamical mass transfer in the BSE algorithm at all times, both when conducting population synthesis and within the N-body code.

An alternative approach to setting up the orbital parameters of the primordial binaries is to use the method of pre-MS tidal evolution developed by Kroupa (1995b). Here it is assumed that the majority of low-mass stars form in aggregates that dissolve within 10 Myr (Kroupa 1995a) and that correlations between orbital parameters observed for short-period systems are the result of evolution in young binaries (less than 10^5 yr) as the two accreting protostars interact. A birth period distribution can be constructed following Kroupa (1995b) and tidal evolution is imposed on the eccentricity to replicate the observed deficiency of eccentric orbits for short-period G dwarfs. A correlation between the masses of the binary stars is also noted (Kroupa 1995b). To investigate how this affects the production of BSs we set up the primordial binaries in the following manner. First the binary mass is chosen from the IMF of Kroupa, Tout & Gilmore (1991) and the component masses are set by choosing a mass ratio from a uniform distribution. This is the same method as used by Hurley et al. (2001) when they assumed correlated masses for the binary stars. Next a period is chosen according to the distribution given by Kroupa (1995b, equation 8) but with the generating function given in Kroupa (1995a, equation 11b) with $\delta = 2.5$, $\eta = 45$ and $\log P_{\rm min}/{\rm d} = 0$. This gives $\log P_{\rm max}/{\rm d} = 8.43$ for the distribution. An eccentricity is then chosen from a thermal distribution (Heggie 1975). If the periastron distance, $R_{\rm peri}$, for these parameters is less than five times the ZAMS radius of the primary, because pre-MS stars can typically be of this size (Kroupa 1995b), it is assumed that a collision would have occurred during the initial evolution and a new set of parameters is chosen. When this test is passed the birth eccentricity, $e_{\rm b}$, is modified according to tidal evolution by

$$\ln e_{\rm i} = -\left(\frac{\lambda R_\odot}{R_{\rm peri}}\right)^\chi + \ln e_{\rm b} \qquad (1)$$

(Kroupa 1995b: equations 3b and 4), where $\lambda = 28$, $\chi = 0.75$ and $e_{\rm i}$ is the resulting eccentricity of the primordial binary.

Generating up 500 000 binary stars and evolving them with the BSE algorithm we find that only 1.5 BSs per 10 000 primordial binaries are predicted at 4 Gyr. This is in contrast to the model of Hurley et al. (2001) which predicts 11 BSs per 10 000 primordial binaries. Furthermore all of the tidally modified BSs are in wide circular binaries – no Case A or Case B mass transfer occurred. Recently Davies, Piotto & De Angeli (2004) have claimed that primordial binaries make mostly BSs in wide binaries and that the Case A/merger scenario is not dominant. This is based on the Preston & Sneden (2000) observations of field blue metal-poor (BMP) stars. However, from the Preston & Sneden (2000) data, it seems that if we assume that all BMP stars are BSs, then a possible mix of these BSs is 40 per cent from Case A evolution (single BS), 10 per cent from Case B (BS in short-period binary) and 50 per cent from Case C evolution (BS in wide binary). Furthermore, about 50 per cent of the wide binaries containing a BMP star have eccentric orbits and a possible explanation of these is that the BMP star (or BS) formed when the two stars comprising the inner binary of a triple merged. This would indicate that a large fraction of BMP stars were formed via the Case A/merger path. All we say on this for now is that much more could be done to constrain parameter distributions using population synthesis in combination with data from field stars and open cluster populations. We plan to look at this further in the near future.

We will proceed with the Kroupa (1995b) tidal evolution method, as described above, to generate the primordial binary population of our Model 1. This predicts about one BS from the primordial binaries so in effect the cluster environment must do all the work to create the observed population. Even though we expect that this will not be the case it is of interest to see if the dynamics can do it alone.

In the previous section we mentioned that we will also evolve a second model which will start with more stars than Model 1 and orbit at a closer distance to the Galactic centre (see Section 6 for details). For this model we also want the primordial binaries to be expected to produce BS numbers of the order of what is observed in M67. The way we select the masses stays the same, $M_{\rm b}$ from Kroupa, Tout & Gilmore (1991) and $n(q) = 1$. However, instead of using the Kroupa (1995b) period distribution we simply select the initial separation from a flat distribution of $\log a$ and impose an upper cutoff at 50 au. For a binary with $M_{\rm b} = 1 M_\odot$ this corresponds to a period of 1.3×10^5 d. A population of 50 per cent binaries chosen in this way actually represents

[2] The wind velocity parameter, β was reduced from 1/2 to 1/8 with the lower value more in keeping with observations

a population of 100 per cent binaries if all periods out to $\log P_{\rm max}/{\rm d} = 8.43$ are allowed, as in Model 1. The assumption then is that all binaries born with $a > 50\,{\rm au}$ quickly disassociate by weak encounters with other stars. Ignoring these non-interacting binaries of low binding energy will not affect the evolution of the cluster or the formation of stars such as BSs. At the lower end of the separation distribution we reject any that is less than twice the sum of the ZAMS radii of the component stars. We then choose an eccentricity from a thermal distribution (Heggie 1975), as before, and modify it according to the Kroupa (1995b) tidal evolution test (Eq. 1) if necessary. We note that Kroupa (1995a) claims that a flat distribution of $\log P$ is consistent with pre-MS orbital data and that the Duquennoy & Mayor (1991) survey of binaries in the solar neighbourhood with G-dwarf primaries does not rule out a flat distribution of $\log a$. Evolving 500 000 binaries set up in this way with the BSE algorithm gives 21 BSs at 4 Gyr per 10 000 primordial binaries. The population synthesis predicts that 75 per cent of these should be single, 13 per cent in short-period circular binaries, and the remaining 12 per cent in wide circular binaries. Thus the interest for Model 2 is in seeing if the combination of the cluster environment and the evolution of the primordial binaries can put the BSs in the required mix of living arrangements, while also maintaining the expected number of BSs.

4 SIMULATION METHOD

We use the `NBODY4` code (Aarseth 1999) to model the dynamical evolution of star clusters. Basic integration of the equations of motion is performed by the Hermite scheme (Makino 1991) which employs a fourth-order force polynomial and exploits the fast evaluation of the force and its first time derivative by the GRAPE-6 (Makino et al. 2003). A time-step scheme comprising a series of hierarchical levels (McMillan 1986) allows each star to evolve on its own natural dynamical timescale while forcing a block of particles to be advanced at each cycle so that efficiency does not suffer. Also, only one prediction is required for each block step. Regularization techniques are used to treat perturbed two-body motion in an accurate and efficient manner (Mikkola & Aarseth 1998) with an extension to chain regularization (Mikkola & Aarseth 1993) to deal with compact subsystems of up to six bodies. A semi-analytical criterion developed by Mardling & Aarseth (2001) is utilized to detect and evolve stable hierarchical triple and quadruple systems which otherwise would prove extremely time consuming by direct integration. Exchange interactions in encounters between single stars and binaries, or binary-binary encounters, where the member of a binary is displaced by an incoming star are included in this treatment. Direct collisions between stars (Kochanek 1992) and the formation of binaries in three- and four-body encounters are also allowed. Binary orbits may also become chaotic owing to perturbations from nearby stars and this scenario is modelled using the Mardling & Aarseth (2001) algorithm.

In `NBODY4` stellar and binary evolution are performed in step with the dynamical evolution so that interaction between these processes is modelled consistently (Hurley et al. 2001). Stellar evolution is included in the form of the single star evolution (SSE, Hurley, Pols & Tout 2000) algorithm. This is a package of analytical formulae fitted to the detailed models of Pols et al. (1998) that covers all phases of evolution from the ZAMS up to, and including, remnant phases. It is valid for masses in the range $0.1 - 100 M_\odot$ and metallicity can be varied. The SSE package contains a prescription for mass loss by stellar winds that is utilized in `NBODY4`. It follows the evolution of rotational angular momentum for each star after the ZAMS spin orbital period is assigned according to a fit to the rotational velocity data of Lang (1992). All aspects of standard binary evolution are treated according to the BSE algorithm (Hurley, Tout & Pols 2002). Circularization of eccentric orbits and synchronization of stellar rotation with the orbital motion owing to tidal interaction is modelled in detail. Angular momentum loss mechanisms, such as gravitational radiation and magnetic braking, are also modelled. Wind accretion, where the secondary may accrete some of the material lost from the primary in a wind, is allowed with the necessary adjustments made to the orbital parameters in the event of any mass variations. Mass transfer also occurs if either star fills its Roche lobe and may proceed on a nuclear, thermal or dynamical timescale. In the latter regime the radius of the primary increases in response to mass loss at a faster rate than the Roche lobe of the star. Stars with deep surface convection zones and degenerate stars are unstable to such dynamical timescale mass loss unless the mass ratio of the system is less than some critical value. The outcome is a common-envelope (CE) event if the primary is a giant. This results in merging or formation of a close binary, or a direct merging if the primary is a WD or low-mass MS star. On the other hand, mass-transfer on a nuclear or thermal timescale is assumed to be a steady process. Prescriptions to determine the type and rate of mass transfer, the response of the secondary to accretion and the outcome of any merger events are in place in BSE and the details can be found in Hurley, Tout & Pols (2002).

One aspect that we should elaborate on here is the modelling of blue stragglers within BSE (and by association `NBODY4`). If a MS star accepts mass from another star then it is rejuvenated. How this is done depends on whether the MS star has a radiative core ($0.35 \leqslant M/M_\odot \leqslant 1.25$), a convective core ($M > 1.25 M_\odot$) or is fully convective ($M < 0.35 M_\odot$). As a MS star gains mass it evolves up along the MS to higher luminosity and effective temperature. If the core is radiative the fraction of hydrogen that has been burnt is only slightly affected so that the effective age of the star decreases. In practice the age of the star is altered so that the fraction of its MS lifetime that has elapsed is unchanged by the change of mass. For MS stars with convective cores, and fully convective stars, the core grows and mixes in unburnt fuel as the star gains mass, so that the star appears even younger. The rejuvenation process is approximated by conserving the amount of burnt hydrogen and assuming that the core mass grows directly proportional to the mass of the star. We then take the remaining fraction of MS lifetime to be directly proportional to the remaining fraction of unburnt hydrogen at the centre to set the new effective age of the star. Owing to the increase in mass the remaining MS lifetime of the star has been reduced but it has been rejuvenated relative to other stars of its new mass.

The merger or collision of two MS stars produces a new

MS star and we assume that the stellar material is completely mixed in the process, with no mass lost from the system. The age of the new star is calculated on the assumption that, as stars evolve across the MS core hydrogen burning proceeds uniformly and that the end of the MS is reached when 10 per cent of the total hydrogen has been burnt. These stars are also rejuvenated relative to other stars of the same mass. The process of rejuvenation and subsequent evolution of the MS star are most likely adequate in the case of steady mass transfer although there is a lack of detailed studies to confirm this (Sills et al. 2003). The assumption that no mass is lost in a collision is in fair accordance with smoothed-particle hydrodynamics simulations of low-velocity collisions (Sills et al. 2001), but only a limited amount of mixing is found in these simulations so our assumption of complete mixing is questionable, and even more so in the case of slow mergers. In addition, the collision product is not initially in thermal equilibrium and requires a thermal timescale to contract to its MS state. During this time it has a higher probability to undergo additional interaction (Lombardi et al. 2003). Furthermore the collision or merged product is, in most cases, rapidly rotating and needs to lose angular momentum in order to contract (Lombardi, Rasio & Shapiro 1996). These effects are not considered in our simplified model of post-collision BSs but would have an effect on the appearance of these stars.

The great advantage of having the identical stellar and binary evolution algorithms in an N-body code and a population synthesis code is that we can evolve the same populations inside and outside the cluster environment to quantify how the dynamical evolution affects the stellar populations. N-body simulations presented in this work were conducted on the 32-chip GRAPE-6 boards (Makino 2002) located at the American Museum of Natural History.

5 RESULTS FOR MODEL 1

The cluster of 9 000 single stars and 9 000 binaries set up in the manner described in Sections 2 and 3 was evolved from zero-age to an age of 5.8 Gyr when 1 000 stars remained. This simulation took approximately one month to complete. Figure 2 shows the mass profile of the simulated cluster after 4 Gyr of evolution. The mass remaining in the cluster at this time is $3\,175 M_{\odot}$. It is contained within a tidal radius of 21 pc. We note that the mass profile does continue beyond the tidal radius because stars are not removed from the simulation until their distance from the density centre exceeds twice that of the tidal radius (cf. Terlevich 1987; Giersz & Heggie 1994). For this particular model the mass exterior to the tidal radius is $84 M_{\odot}$, or 2.7% of the total mass. Also shown in Figure 2 is the mass profile for the luminous mass which amounts to $1\,987 M_{\odot}$. The luminous mass, that in stars above $0.5 M_{\odot}$ burning nuclear fuel, contained within 10 pc is $1\,730 M_{\odot}$ and it has a half-mass radius of 3.0 pc. The half-mass radius for all stars is 4.9 pc. Fan et al. (1996) determined a luminous mass for M67 of $1\,016 M_{\odot}$, rising to $1\,270 M_{\odot}$ when corrected for binaries, for stars within 10 pc of the cluster centre. Our model has too much mass remaining to be a good representation of M67. It is not until 5.2 Gyr that we find $M_{\rm L} = 1\,000 M_{\odot}$ and we consider this too old to be relevant to M67. General results for this model are summarized in Table 2.

At 4 Gyr the model contains only one blue straggler. This star resides in a non-primordial binary with an orbital period of 83 d and an eccentricity of 0.5. The mass of the BS is $1.5 M_{\odot}$ – compared to $M_{\rm TO} = 1.32 M_{\odot}$ – and the companion is a $0.64 M_{\odot}$ MS star. Slightly earlier (3 950 Myr) there were two BSs and slightly later (4 050 Myr) there are three, so an average of two BSs at this age. The most BSs observed in the cluster at any one time, from an age of 3 Gyr onwards, is 5 at 4.5 Gyr. So the combination of the Kroupa (1995b) setup for the primordial binaries and the dynamical evolution of the cluster does not explain the actual M67 BS population. This is not a quirk of the model, either in terms of the initial conditions or statistics. We have performed a variety of simulations with the primordial binaries chosen in the same manner but have altered various characteristics of the starting model such as the King model for the density profile and the tidal radius filling factor. These models were evolved as part of a broader project to understand the evolution of binary-rich open clusters and will be described in detail in a forthcoming paper. In none of these models did we see substantial BS production. It has been noted previously (Giersz & Heggie 1994) that statistical fluctuations in N-body models may be reduced by averaging over the results of many simulations. These fluctuations are amplified for small N and should not be of major concern in models of the size presented here (compared to the $N = 500$ models discussed by Giersz & Heggie 1994). However, we have repeated Model 1 with an identical set up except for a different seed for the random number generator. The evolution is similar – the mass remaining in the cluster after 4 Gyr is $2\,957 M_{\odot}$ within a tidal radius of 20 pc and the luminous mass within the central 10 pc is $1\,692 M_{\odot}$. At no time subsequent to an age of 3 Gyr are more than five BSs found in the model cluster. Therefore the nature of the primordial binaries in this type of simulation does not seem appropriate for a model of M67. Rather than continuing further with our analysis of Model 1 we instead turn our attention to Model 2.

6 RESULTS FOR MODEL 2 – THE M67 MODEL

A flaw of Model 1 was that it contained too much mass at 4 Gyr to be considered a good model of M67. One way to reduce the mass remaining in a cluster at a certain age is to increase the strength of the tidal field in which the cluster evolves (Vesperini 1997; Baumgardt 2001). This reduces the tidal radius of the cluster which leads to an increase in the escape rate of stars. Associated with the reduction in mass is a lowering of the relaxation timescale (typically the half-mass radius will also be smaller) so that the cluster is dynamically older for a given physical age. The parameters given for the orbit of M67 in the Galaxy (Carraro & Chiosi 1994) indicate an eccentricity of 0.14 and a time-averaged semi-major axis of 8 kpc. So, when evolving Model 2, we will place the cluster on an orbit at 8.0 kpc from the Galactic centre. An orbital speed of $220\,{\rm km\,s^{-1}}$ is still applicable at this distance (Chernoff & Weinberg 1990) so this remains unchanged and we keep the cluster on a circular orbit.

With the stronger tidal field we now expect the mass remaining after 4 Gyr of evolution to be less than that found for Model 1 and closer to the mass of M67, as desired. However, we anticipate that the shorter relaxation time will drive the evolution faster than required to give the desired 25% reduction in cluster mass. So we make an associated increase in the particle number of the starting model to 12 000 single stars and 12 000 binaries. This gives $M_0 = 18\,700 M_\odot$ within a tidal radius of 32 pc.

The only other change in Model 2 compared to Model 1 is in the set-up of the primordial binary population. As discussed in Section 3 a flat distribution of $\log a$ will be used to generate the orbital separations of the primordial binaries. This has a cutoff at 50 au which is comparable to the hard-soft binary limit (Heggie 1975) of about 40 au for Model 2 with an initial half-mass radius of 3.9 pc. In all other respects the set up for Model 2 is the same as for Model 1. The two starting models are compared in Table 1. From the 12 000 primordial binaries in Model 2 we should expect 25 BSs from binary evolution alone (see Section 3).

The mass profile for Model 2 at 4 Gyr is shown in Figure 3. It has a total mass of $2\,037 M_\odot$ and a luminous mass of $1\,488 M_\odot$ within a tidal radius of 15 pc. The luminous mass within 10 pc of the cluster centre ($M_{\rm L,10}$) is now $1\,342 M_\odot$ which compares well with the binary corrected value found by Fan et al. (1996). Slightly later in the evolution (4.1 Gyr) the model has $M_{\rm L,10} = 1\,181 M_\odot$ with a tidal radius of 14.5 pc. The half-mass radius of MS stars observed within 10 pc was determined by Fan et al. (1996) to be 2.5 pc and our model has 2.7 pc for the same set of stars. So we now have a good match to the observed mass of M67 as well as the half-mass and tidal radii. General results for this model are summarized in Table 2.

In Figure 4 we once again show the mass profiles at 4 Gyr but this time normalized to the total mass of each profile. The luminous mass is more centrally concentrated. Naively this result would be expected owing to mass-segregation when we consider that low-mass MS stars are excluded from the luminous mass. However, the effect is counteracted somewhat by the added exclusion of white dwarfs (WDs) from the luminous mass because these are generally born in the central regions of the cluster and themselves are centrally concentrated relative to the entire population. Also shown in Figure 4 is the normalized mass profile of the BSs of which there are 20 in the model at 4 Gyr. These are more likely to be found in the centre of the cluster and have a half-mass radius of 1.1 pc. Fan et al. (1996) determined a half-mass radius of 1.6 pc for the M67 BSs. We elaborate further on the BSs and other stellar populations in Section 6.2.

The cluster at 4 Gyr of age is a dynamically relaxed system – 13 half-mass relaxation times have elapsed in reaching this point. Figure 5 shows the behaviour of the number density of stars contained within the core and the half-mass radius of the cluster as it evolved from 0 to 4 Gyr. The core density of the starting model was 150 stars pc^{-3}. This rose to a maximum of 330 stars pc^{-3} after 3.5 Gyr. Here the core radius is the density-weighted value commonly used in theoretical models (Casertano & Hut 1985; Aarseth 2003) which is typically smaller than the core radius determined from observational techniques (Wilkinson et al. 2003). For binary-rich clusters there is no clear core collapse, at least not to the extent that we witness in simulations without primordial binaries, where a high core density is required for binary formation (e.g. Hurley et al. 2004). Heating of the core by binaries occurs from the beginning in simulations with a large primordial binary population and this helps to keep the evolution of the core radius relatively regular and to avoid extreme fluctuations in central density. Stellar evolution mass-loss also leads to core expansion, especially at early times when massive stars evolve away from the MS. The core density of the model at 4 Gyr is 83 stars pc^{-3}. The density of stars contained within the half-mass radius started at 50 stars pc^{-3} and evolved to 4 stars pc^{-3} at 4 Gyr. Hence this was not a particularly dense system. At an age of 5 Gyr the model cluster contains only 200 stars with a total mass of $260 M_\odot$ and has almost reached the point of complete dissolution. In this paper the focus is on the results of the simulation at the age of M67 and the relevance of the model in improving our understanding of the observed properties of M67. We do not dwell on the details of the simulation in reaching an age of 4 Gyr. We shall present the long-term evolution of a binary-rich star cluster in another paper (Hurley et al., in preparation).

6.1 Cluster Structure

The coordinate system used in the N-body simulation has the cluster centre-of-mass as the origin, the X-axis directed away from the Galactic centre, the Y-axis in the direction of rotation about the Galactic centre and the Z-axis normal to the plane of the disk. In order to show how the model of M67 might appear on the sky we have rotated the model according to the Galactic coordinates of M67 ($l = 215.68°$, $b = 31.93°$: Bonatto & Bica 2003) so that the transformed YZ-plane becomes the observed plane (which we have also denoted the yz-plane). This view of the model is presented in Figure 6. .

Bonatto & Bica (2005) used 2MASS data to construct a surface density profile for M67. This is shown in Figure 7. The limiting radius for the observations is 11.7 ± 0.6 pc and fitting a King (1966) surface density profile to the data gives a core radius of 1.14 ± 0.13 pc within a tidal radius of 16 ± 3 pc (Bonatto & Bica 2005). Using the same radial bins as for the observed M67 surface density profile, we also show the profile for the model in Figure 7. The surface density of stars is greater in the model, especially in the central regions. However, the observed profile includes only stars with $J < 14.5$ which corresponds to stars with masses of about $0.8 M_\odot$ or greater. Restricting the model profile to stars in this range, we find that agreement between the model and the observations is better. The match is good in the $1-6$ pc range which is the region that contains the half-mass radius of the cluster. Exterior to 6 pc the observed surface density drops to levels similar to that of the background counts (about 1 star pc^{-2}) so it is not significant that the model surface density is lower in this region. We note that background contamination is nil in the N-body model. At the centre the model surface density is still too high. The model is overdense by a factor of 3 in the central bin. Fitting a King (1966) surface density profile to the model data gives a core radius of 0.6 pc so the model is clearly more centrally concentrated than observations indicate for M67. Saturation effects could be lowering the observed star counts in the core of M67 but this is not expected to be significant. We note that there is no noticeable

change in the model profile if we use different projections to construct it.

A common method used in the analysis of observed cluster data is to construct a surface brightness profile. This can also be done with the N-body cluster data for which the mass, luminosity, stellar radius and position of each star is known, as well as whether or not the star is in a binary. First we calculate magnitudes and colours for each star using bolometric corrections provided by Kurucz (1992) and, in the case of WDs, Bergeron, Wesemael & Beauchamp (1995). Then the magnitude and position information is passed through the pipeline described by Mackey & Gilmore (2003) in their analysis of LMC clusters to give a projected surface density profile. The resulting data points for our M67 model for the V-band in the XZ-plane are shown in Figure 8. A fit of the three-parameter Elson, Fall & Freeman (1987) model to the cluster profile is also shown and this gives a core radius of 0.66 pc. In this case all stars have been considered and the data is rather noisy. If we repeat the process but remove all stars with $V < 12$ in order to reduce saturation effects by bright stars and also remove all stars with $V > 17$ to mimic a faint detection limit then we get the much cleaner profile shown in Figure 9. The fit to these data points gives a core radius of 0.64 pc.

6.2 Stellar populations

In Figure 10 we present the colour-magnitude diagram (CMD) of Model 2 at 4.0 Gyr. There are 870 single stars and 1 325 binaries in the cluster at this time. The MS turn-off mass is $1.32M_{\odot}$. The cluster contains 2 968 MS stars, 57 giants and subgiants, 2 naked helium (nHe) stars, 491 WDs and 2 neutron stars. Defining BSs as MS stars with mass in excess of the MS turn-off mass (by 2% or more) we find 20 with masses in the range $1.4-2.1M_{\odot}$. These form the group of stars blueward of the the MS in the CMD. Nine of the BSs are in binaries. The BS population is discussed in detail in Sect. 7.2.1. There are six RS Canum Venaticorum (RS CVn) stars in the cluster. These are binaries with periods of $1 \leqslant P/\mathrm{d} \leqslant 14$ that contain a cool subgiant star and a MS companion (Hall 1976). They are believed to be sources of X-ray emission. These and other expected X-ray sources in the cluster are discussed in Sect. 7.2.2.

In the cluster at 4 Gyr are 226 single WDs. Most of these lie on the distinctive WD cooling track seen in the lower left corner of the CMD. There are 60 double-WD binaries, the majority of which are found in the CMD by their position above the sequence of standard single WDs. Of the double WDs, 28 have periods less than 1 d. The stars appearing in the region between the WD sequence and the MS are WD-MS star binaries in which the WD is still young and fairly hot. As the WD cools the binary moves across the CMD towards the MS as the MS star begins to dominate the appearance of the binary. Further particulars of the WD population are discussed in Sect. 7.2.3. There is also one cataclysmic variable (CV) in the cluster at this time, located at $V = 23.06$ and $(B-V) = 0.53$ in the CMD. It comprises a $0.1M_{\odot}$ MS donor star in a 0.55 d circular orbit with a $0.3M_{\odot}$ helium WD. The CV phase began at an age of 1.9 Gyr when the MS star mass was $0.18M_{\odot}$.

A summary of selected stellar population results for the M67 model is given in Table 3 along with results from Model 1. There are two extremely blue stars at $V \approx 12$ in the CMD. These are not BSs but binaries comprised of evolved nHe stars with MS star companions. Both evolved from primordial binaries in which the nHe star was produced in a CE event initiated by the progenitor of the nHe star filling its Roche lobe while on the early AGB. However, the fainter of the two binaries would not exist in this state without having experienced a significant perturbation to its orbit. It originated as a primordial binary with an eccentricity of 0.5 and a period of 30 902 d. Evolved in isolation the two stars would not have become close enough to interact and the result would be a WD-MS star binary with an orbital period of about 300 yr at 4 Gyr. Within the cluster environment the binary received a perturbation to its orbit from a third star, in a flyby encounter after 350 Myr, while still a MS-MS star binary. This resulted in a slight decrease in orbital period but more important pumped the eccentricity up to 0.95 and subsequent tidal evolution brought the stars close enough for mass-transfer to begin. The CE event then reduced the orbital period further so that the nHe-MS star binary observed at 4 Gyr has $P = 12.6$ d and is circular. The other nHe-MS star binary has a period of 3.5 d.

Another anomalous star in the CMD lies towards the base of the giant branch (GB) but below the subgiant branch at $V = 13.32$ and $(B-V) = 0.83$. This is a single star with a mass of $1.91M_{\odot}$ recently created in a CE merger event. At an age of 3.8 Gyr a $1.37M_{\odot}$ subgiant primary filled its Roche lobe and began steady Case B mass transfer on to its $0.83M_{\odot}$ MS star companion. When the primary reached the end of the subgiant phase (about 50 Myr later) its mass had been reduced to $0.98M_{\odot}$ and the companion mass was $1.22M_{\odot}$ owing to the mass-transfer being conservative. At this stage the envelope of the primary was fully convective and the entire envelope overflowed the Roche lobe on a dynamical timescale to create a common envelope. The mass ratio inversion had not been enough to avoid this. The giant core and the MS star spiralled together and expelled $0.29M_{\odot}$ of the envelope via dynamical friction before merging to form a $1.91M_{\odot}$ giant with a core mass of $0.16M_{\odot}$. This star is more massive than the normal giants in the cluster at this time but has a core mass less than expected for a giant of this mass and in fact less than the core mass of the stars residing at the base of the cluster GB. The reduced core mass is the result of the mass loss experienced by the subgiant progenitor which restricted its core mass growth as it evolved across the subgiant branch. This is the cause of the merged giant lying below the subgiant branch. The increased mass of the giant will cause it to remain on the blue side of the standard cluster GB as it continues its giant evolution.

6.2.1 Blue stragglers

Table 4 provides a list of the 20 BSs in the M67 model. All of the eleven single BSs were produced from the merger of two MS stars in a primordial binary. In nine of these cases BS formation was via the onset of Case A mass-transfer and the eventual coalescence of the stars as angular momentum was removed from the system. For seven of these the evolution proceeded as if the binaries were evolved in isolation. The cluster environment did not interfere. In one case (star #2411), a perturbation to the orbit hastened the onset of

Case A mass-transfer so that a BS that would not have been created until after 4 Gyr was formed earlier and observed at 4 Gyr. In another case (#3021) mass transfer was delayed by the involvement of the binary in a temporary exchange interaction which increased the orbital period. This BS would not have been observed at 4 Gyr without the interference of the third star as it would have already evolved to become a WD. On the other hand, if the exchange interaction had caused a larger period increase the BS may have formed after 4 Gyr or not at all. The remaining two of the single BSs formed from initially long-period binaries that had their eccentricity pumped up to 0.99 by weak flyby encounters. This led to a collision of the MS star components at periastron and creation of a BS. In neither binary would the component stars have become close enough to interact and merge without the intervention of a third star. Descriptions of the evolution pathways for the four single BSs that were affected in some way by the cluster environment are given in Table 5.

Descriptions for the nine binary BSs are also given in Table 5. Two of these are primordial binaries but both have been affected by interactions with other cluster members. This explains the eccentric nature of the orbits. In one case the BS was formed in a wide circular binary as a result of Case C mass-transfer and a subsequent perturbation induced the eccentricity observed in the orbit. The other primordial binary became involved in a four-body interaction and one of the binary components collided with another member of the subsystem to form the BS which then emerged bound to its original companion. The remaining BS-binaries are non-primordial and their formation involved an exchange interaction at some point. In four of these cases a primordial binary became part of a three- or four-body system and perturbations to the orbit drove the eccentricity of the binary towards unity so that the stars collided. The merged star, a BS, was then exchanged into a binary. One of these cases then underwent a second collision in an eccentric binary while another was subsequently perturbed. A BS binary was formed from Case-C mass transfer in a primordial binary but the BS was then exchanged into a new binary and, just prior to 4 Gyr, Case B mass-transfer began in this binary. This further increased the mass of the BS. Another case saw an exchange interaction form a binary which evolved to a state of Case-A mass transfer followed by coalescence to a BS which was later exchanged into a new binary. The final case involved an exchange interaction followed by two collision events. So the binary BSs were formed by a variety of means and this resulted in a mix of orbital parameters: short-period and circular, short-period (less than 1 000 d) and eccentric, long-period (greater than 1 000 d) and eccentric (see Table 4 for full details).

Only seven of the 20 BSs in the model evolved from unperturbed primordial binaries. Of the remaining 13, eight BSs were formed by collisions that were induced by three- or four-body interactions, or by perturbations that drove up the eccentricity to almost unity. These eight could not have formed outside the cluster environment and the same is true for the case A merged star that formed after an exchange. The other four would have become BSs by binary interaction alone but two of these would not have been observed as BSs at an age of 4 Gyr. Hence, for approximately half the BS population the dynamical cluster environment was instrumental in producing them.

As mentioned earlier the half-mass radius for the BSs in the M67 model is 1.1 pc. This is much less than the half-mass radius for all stars (3.8 pc) and indicates that the BSs are a centrally concentrated population which is in agreement with their observed distribution in M67 (Fan et al. 1996). The fact that BSs are more likely to be found in the centre of the cluster than the outer regions is confirmed by Figure 11 which splits the CMD into two regions, stars contained within the half-mass radius and stars exterior to this. We see that only two of the BSs in the model at 4 Gyr are found outside of the half-mass radius and one of these was situated well within the half-mass radius when it formed[3]. The reasons for this are twofold. Primordial binaries which are to produce a BS must have a mass in excess of the current MS turn-off mass ($1.3M_{\odot}$) which itself is greater than the average mass of the cluster stars ($0.6M_{\odot}$). So the process of mass-segregation acts to concentrate these binaries at the centre of the cluster and the BSs themselves, when created, also tend to sink towards the centre. We also have BSs created in binaries formed from exchange interactions and these interactions are more likely in regions of high density (Heggie, Hut & McMillan 1996) which favours the centre of the cluster (see Figure 5).

The 20 BSs in the model at 4 Gyr is less than the 25 predicted when evolving the primordial binaries in isolation (see Section 3). Considering that only 11 of the 20 BSs would have formed without help from the cluster environment, this means that 14 potential BSs at 4 Gyr were lost during the simulation. So in addition to creating BSs the cluster environment is just as productive in destroying potential BSs, maybe even more so. The majority of *lost* BSs were the result of perturbations to primordial binaries that hardened the orbit and brought forward the onset of Case-A mass transfer. BS formation still occurred in these binaries but much earlier than it would have otherwise and this caused the BS phase to have ended prior to 4 Gyr. This is compensated to some extent by somewhat wider binaries being hardened into orbits that allow them to experience Case-A mass transfer and coalesce but otherwise would not have done so within 4 Gyr, and by interactions that delay the onset of mass transfer as in the case of #3021. Other possibilities include an exchange interaction destroying the primordial binary or the binary being ejected from the cluster. Both of these events are rare compared to the hardening scenario. The former because the pre-exchange binary is short-period and the latter because the binary is relatively heavy.

There are no BSs in long-period (nearly) circular binaries present at 4 Gyr whereas there are two observed in M67: $P = 1\,221$ d, $e = 0.09$ and $P = 1\,154$ d, $e = 0.07$ (Latham & Milone 1996). However, BSs in such binaries were present in the simulation at other times. An example is a $1.8M_{\odot}$ BS in a circular orbit of period 1 445 d with a WD companion at 2.6 Gyr. The proto-BS initially accreted mass from

[3] This BS lies outside of the tidal radius at 4 Gyr, 19.4 pc from the cluster centre. It is counted as a cluster member because its orbit is such that it remains bound to the cluster and subsequently returns within the tidal radius. The particulars of this BS are provided in Table 4 (BS #2565) and its evolution pathway is detailed in Table 5. The radial position of this BS explains why the normalized mass profile of the BSs in Figure 4 does not reach unity within the tidal radius.

the stellar wind of its AGB-star companion and then grew even more in mass with the onset of Case-C mass transfer, with dynamical timescale mass-transfer and CE evolution avoided because the stellar wind had significantly decreased the mass of the AGB star by this stage. Mass transfer ceased when the AGB star exhausted its envelope and became a WD. Also, BS #1378 observed at 4 Gyr in a long-period eccentric binary was originally in a wide circular binary when formed at $T = 2$ Gyr. It would have been found in this state at 4 Gyr if the orbit had not been perturbed by a passing star at 2.5 Gyr. So in a sense it is simply bad luck that we did not observe any BSs in long-period circular binaries after 4 Gyr of evolution. The same can be said for the incidence of super-BSs. M67 is observed to have a super-BS of mass $3M_{\odot}$ (Leonard 1996) but our model at 4 Gyr does not contain any BSs with mass greater than twice the MS turn-off mass of the cluster. Super-BSs do form in the simulated cluster, a total of five for the entire simulation including one at 3.9 Gyr when the model contained 22 BSs. This super-BS of mass $3.2M_{\odot}$ was found in a binary of period 4.6 d and eccentricity 0.45 with a $1.2M_{\odot}$ MS star companion. The star began its life as a $1.2M_{\odot}$ MS star with a $1.3M_{\odot}$ companion in a circular primordial binary with $P = 1.2$ d. After 2.7 Gyr the more massive MS star filled its Roche lobe and Case-A mass transfer proceeded until 3.1 Gyr when the stars coalesced to form a $2.5M_{\odot}$ single BS. The BS was situated well within the core of the cluster (0.1 pc from the centre) and at 3.4 Gyr exchanged itself into an existing binary. Its new companion was a $0.7M_{\odot}$ MS star and the orbit had an eccentricity of 0.1 and a period of 1.3 d. The orbit quickly circularized owing to tidal forces and Case-A mass transfer began at 3.6 Gyr with coalescence almost immediately afterwards. This newly formed $3.2M_{\odot}$ super-BS was exchanged into a wide binary with a $1.3M_{\odot}$ companion at 3.7 Gyr and this binary was then involved in a short-lived four-body system that created the short-period eccentric binary observed at 3.9 Gyr. The super-BS evolved off the MS about 50 Myr later and just missed being included in the M67 model. This evolution example also serves to highlight how BSs may be formed in short-period eccentric binaries. M67 is observed to contain a BS in an orbit with period 4.18 d and eccentricity of 0.2 (Milone & Latham 1992).

The orbital parameters of all BS–binaries created in Model 2 at an age of 2 Gyr or later are shown in Figure 12. Also shown are the six M67 BS-binaries with known orbital solutions. Figure 13 shows the total number of BSs and BSs within binaries as a function of cluster age up to 4.2 Gyr. We note that the numbers we have focussed on at 4 Gyr are typical of the cluster over the preceeding Gyr or so. The increase in BS number seen after 2 Gyr corresponds to an increase in central density as the cluster becomes dynamically more evolved. The BSs found in binaries during this timeframe are more likely to be in non-primordial binaries which is the opposite of what is found earlier in the evolution. In Figure 13 we also show the number of BSs in circular binaries with $P < 100$ d. Only one BS binary of this type is found in the cluster at 4 Gyr but at earlier ages these binaries, formed primarily from Case B mass transfer, were dominant. Of the BS binaries formed prior to an age of 2 Gyr 82 per cent were circular with an orbital period of 100 d or less which contrasts with 23 per cent of the BS binaries in Figure 12 being of this type. The number of these binaries declines with age and this is linked to the destruction of primordial binaries as the cluster ages.

We have seen that formation scenarios for all of the various BSs observed in M67 exist in Model 2. The model at 4 Gyr has a binary fraction of about 0.5 for the BSs which is close to the fraction of 0.6 observed. Also, the ratio of BSs to the number of MS stars within two magnitudes of the MS turn-off ($13 < V < 15$) is 0.18 which matches well with the observed value of 0.14 (Ahumada & Lapasset 1995). In fact this indicates that the model is over-producing BSs although if we look at raw numbers the model has 20 BSs at 4 Gyr compared to 28 for M67 (Hurley et al. 2001). However, if we look at the CMD of M67 (e.g. Fig. 2 of Hurley et al. 2001; Montgomery, Marschall & Janes 1993) the BSs appear to form two distinct groups, an obvious group of 10 BSs with $V < 12$ and the remainder much closer to the MS turn-off position. Some of these less obvious BSs actually lie below the MS turn-off by almost a magnitude. The observed BSs are identified by their position in the CMD whereas in the *N*-body model we have much more information about the stars and have used mass as the determining factor. Inspection of Figure 10 and comparison with the positions of the observed M67 BSs reveals that there are at least five stars near the MS turn-off of the model that we may have classified as BSs if using CMD position as the determining factor. Counting these stars as BSs would give good agreement of raw BS numbers for the model and M67. Also, two of the M67 BSs have proper motion membership probabilities of less than 80 per cent (Girard et al. 1989).

We now focus on a comparison with the group of ten M67 BSs with $V < 12$. This sample has been well studied by Milone & Latham (1992) revealing that six are single and four are in binaries. The orbital parameters of the BS-binaries are $P = 4.2$ d and $e = 0.2$, $P = 846$ d and $e = 0.5$, $P = 1\,003$ d and $e = 0.3$, and $P = 1\,221$ d and $e = 0.1$. The simulated cluster at 4 Gyr also has a pronounced group of 15 BSs (those with $|B - V| < 0.45$ in Figure 10). Eight of these are single and seven are in binaries. If we further restrict this sample to $V < 12$ then we have eleven BSs with six in binaries. The widest of these six (#1613 and #3835) may not be detected as having a companion if observed so the mix of BSs in this sample could easily switch to 7 single BSs and 4 binary BSs. Either way, considering the stochastic nature of BS formation, the number of BSs in the restricted sample is a good match to that of the observed group of BSs as is the ratio of single BSs to binary BSs and the orbital combinations of the binary BSs.

6.2.2 X-ray sources

X-ray observations of old open clusters (van den Berg et al. 2004) and globular clusters (Pooley et al. 2003) have proved to be very efficient at detecting short-period interacting binaries. For open clusters there is a well-defined connection between age and X-ray activity (Randich 1997) where the latter declines with age owing to the spin-down of late-type stars which are initially rapid rotators. Therefore, X-ray detections in a cluster such as M67 are expected to be associated with stars that have been spun up in some way, typically by residing in a short-period binary where the spin period of the star is kept synchronized with the orbital period by tidal forces. An example of such a binary is an RS CVn

system which contains a subgiant and a MS star companion in a short-period orbit. BY Draconis binaries are chromospherically active systems containing a late-type (spectral type F or later) MS star primary with a MS star companion and may also explain X-ray activity in old populations.

A Chandra observation of M67 was recently reported by van den Berg et al. (2004). They detected 158 X-ray sources (with a limiting flux corresponding to an X-ray luminosity of $L_X \approx 10^{28}\,\mathrm{erg\,s^{-1}}$). Optical counterparts that are proper-motion members of M67 were found for 25 sources and a further 12 sources had optical counterparts that are believed to be cluster members based on their position near the lower end of the M67 main sequence. Ten of the proper-motion members are binaries with periods less than 12 d and contain subgiant or MS stars. Approximately six of these appear to be classical RS CVn binaries of which three were detected earlier by Belloni , Verbunt & Mathieu (1998). The twelve sources near the lower end of the MS are possible BY Draconis binaries.

Table 6 lists the parameters of the six RS CVn binaries observed in our M67 model at 4 Gyr. Five of these are the result of standard primordial binary evolution while one (#1568) was formed in an exchange interaction. The number is a good match to the M67 observations although possibly we should not count the system in which the primary is filling its Roche lobe (#2633) or the system with a period of 20 d (#2383) when making the comparison as these fall outside of the classical RS CVn period range as defined by Hall (1976).

To investigate the incidence of BY Draconis binaries we look at all MS-MS binaries where the primary is F-type or later ($M_1 \leqslant 1.0 M_\odot$) and the orbital period is 12 d or less. This cutoff in period is used in observational work (e.g. van den Berg et al. 2004) and is thought to ensure that all binaries in the sample are synchronously rotating at the age of M67. Using the relation between X-ray luminosity and rotation rate, Ω, proposed by Walter (1982),

$$\log L_X/L_{\rm bol} = -3.14 - 0.16/\Omega\,, \qquad (2)$$

where $L_{\rm bol}$ is the bolometric luminosity of a star and Ω is in units of rotations/day, we can estimate an X-ray luminosity for each of the BY Draconis binaries. These are plotted in Figure 14 as a function of orbital period. The upper limit to the X-ray luminosity at any period is given by a $1.0 M_\odot$ star in synchronous rotation with its orbit – to emphasize this we have plotted the behaviour of Equation 2 for such a situation (upper solid line in Figure 14). Correspondingly the lower limit occurs for a $0.1 M_\odot$ star – the lowest mass of star that we considered (see the lower solid line in Figure 14). A small number of systems in our M67 model have L_X less than this lower limit and these are binaries where both stars are less massive than $0.2 M_\odot$ and synchronous rotation is yet to be achieved. We have also included data points for the BY Draconis systems identified by van den Berg et al. (2004) for which orbital periods are known (four of twelve). We find 172 MS-MS systems with $L_X > 10^{28}\,\mathrm{erg\,s^{-1}}$. Also shown in Figure 14 are 19 short-period MS-WD binaries which have X-ray luminosities in this range and for which the WD component has cooled sufficiently that the binary appears near the MS in the CMD.

We have an over-abundance of potential MS X-ray sources compared to the Chandra detections for M67. However, the Chandra pointing involved six CCD detectors with each having an area of $8.4' \times 8.4'$ so that the coverage was only about 1/30th of the full area of M67 (for a tidal radius of $60'$). Also, the sensitivity of the Chandra observations decreases towards the edge of the detector and the limiting luminosity will be greater than $10^{28}\,\mathrm{erg\,s^{-1}}$ for the outer detectors (M. van den Berg, private communication). The centre of the cluster was covered by Chandra so we do not expect the RS CVn sample to suffer greatly from incompleteness as these are relatively massive binaries but BY Draconis binaries will not necessarily reside in the central regions of the cluster, especially those with cool primaries. Therefore there may be a substantial population of these systems yet to be observed.

6.2.3 White dwarfs

Hurley & Shara (2003) used N-body models to conduct a detailed investigation of the behaviour and appearance of the white dwarf population in dense star clusters. They found that the mass fraction of WDs can be significantly enhanced by the dynamical evolution of the cluster – by as much as a factor of 2 in old open clusters. This enhancement is relative to the mass fraction expected if the same populations were evolved with basic population synthesis and with the same stellar and binary evolution algorithms used in the N-body code. A combination of mass segregation and the presence of a tidal field mean that, as a cluster evolves, low-mass MS stars are preferentially stripped from the cluster and the WD mass fraction diverges from that of the field population. We find the same behaviour in our M67 model. The expected WD mass fraction at 4 Gyr is $f_{\rm WD} = 0.1$ when we perform population synthesis on the initial population. However, the M67 N-body model has $f_{\rm WD} = 0.15$ at 4 Gyr. The average mass of the cluster WDs starts high and then decreases with time as progressively less-massive WDs are born. After 1 Gyr the WD average mass is $0.82 M_\odot$ and after 4 Gyr it is $0.64 M_\odot$. On the other hand the average mass of MS stars is $0.52 M_\odot$ for the starting model and initially decreases owing to evolution of the massive MS stars followed by an increase to $0.56 M_\odot$ at 4 Gyr because of tidal stripping. In other words, the average mass of MS stars is nearly constant. Based on these values we would expect the WDs to be preferentially found near the centre of the cluster as a result of mass segregation. This expectation is strengthened when we consider that WDs are born from stars that were previously the most massive MS stars in the cluster. What we observe in our M67 model is that the half-mass radius of the WDs is 0.64 pc which is indeed centrally concentrated when compared to a half-mass radius of 3.8 pc for all stars. If we look at only single WDs the half-mass radius increases to 1.28 pc (for comparison the half-mass radius of the cluster binaries is 0.37 pc). The upshot of all this is that low-mass MS stars are more likely to reside in the outer regions of the cluster and are thus more vulnerable to escape from the cluster than WDs.

Figure 15 shows the variation of WD mass fraction as a function of radial position in the M67 model. We see that the value of $f_{\rm WD}$ depends strongly on which portion of the cluster is observed. Somewhat surprisingly the greatest enhancement compared to the population synthesis value is found in the 6 to 10 pc region, exterior to the cluster half-

mass radius. There is less but noticeable enhancement in the core which should contain a significant population of massive old WDs as well as double WDs and less-massive young WDs. However, the central regions are also dominated by massive stars and binaries of all types which reduces $f_{\rm WD}$. This also means that young WDs move outwards from the centre as they cool. Outside the half-mass radius there is a lack of massive stars and binaries, as well as young WDs (see also Figure 11). This increases the relative mass of the WD population. There is one radial bin near the half-mass radius where $f_{\rm WD}$ is similar to the population synthesis value. Unfortunately the behaviour of $f_{\rm WD}$ in the vicinity of this region is rather erratic and this makes it difficult to suggest that observations to determine $f_{\rm WD}$ should be conducted near the half-mass radius. In fact our results indicate that M67 is dynamically old enough that a measurement of $f_{\rm WD}$ cannot be used to yield information about the IMF. Also shown in Figure 15 is the value of $f_{\rm WD}$ calculated if we ignore WDs in binaries with non-WD companions. So this value corresponds to single WDs and double WDs found on or near the WD sequence in the cluster CMD which are the WDs most likely to be observed in a real cluster.

Richer et al. (1998) derive a WD mass fraction of 0.09 for M67. This is based on finding 85 WDs down to the termination point of the WD cooling sequence (their deep survey reached $V = 25$). Correcting this number for WDs hidden in binaries and taking a 50 per cent binary fraction they estimate that there could be as many as 150 WDs in M67. Assuming an average mass of $0.7 M_{\odot}$ for the WDs and using a calculated total mass of $1\,080 M_{\odot}$ for M67 they arrive at the quoted value of $f_{\rm WD}$. Richer et al. (1998) note that this number appears to be low when compared to the number of giants they observed. Based on a population of 87 giants they expected about 60 WDs with a cooling age less than 1 Gyr but found only 24. Our M67 model contains 226 single WDs, 60 double-WD binaries and 145 WDs in binaries with a non-WD companion. Of the single WDs 54 have a cooling age less than 1 Gyr. There are 22 double WDs with at least one bright component and 33 bright WDs contained in other binaries (some of these with low-mass MS companions may appear near the WD sequence). The model also contains 59 giants which gives an approximate 1:1 ratio of bright WDs to giants if we consider only the single WDs. If our model is to be believed this suggests that the observations of WDs in M67 are incomplete.

Nine double-WD binaries with a total mass in excess of the Chandrasekhar mass ($M_{\rm Ch} = 1.44 M_{\odot}$) and merger timescales owing to gravitational radiation of less than the age of the Galaxy (about 13 Gyr) are produced in Model 2. One of these contains two oxygen-neon (ONe) WDs and three have an ONe and a carbon-oxygen (CO) WD component. The outcome of WD-WD mergers involving an ONe WD is believed to be an accretion-induced collapse (AIC: Nomoto & Kondo 1991) to form a neutron star remnant. This is the assumed outcome when such an event occurs in an `NBODY4` simulation. Mergers of CO-CO WD binaries with $M > M_{\rm Ch}$ are possible causes of Type Ia supernovae (Yungelson & Livio 2000) but may instead lead to AIC and the formation of a neutron star (Saio & Nomoto 1998). Shara & Hurley (2002) found that the incidence of these possible Type Ia events increased by as much as a factor of 10 in the environment of an open cluster. This result was based on simulations of 20 000 stars with a 10 per cent primordial binary population and the Eggleton, Fitchett & Tout (1989) orbital separation distribution used to set up the binaries. From the 12 000 primordial binaries in our simulation, population synthesis with the BSE code predicts that we should get three super-Chandrasekhar CO-CO WD mergers. So the five that we did find represents an enhancement but not of the order found by Shara & Hurley (2002). However, it is too early to tell if the degree of enhancement depends on primordial binary fraction. The two additional CO-CO mergers in Model 2 are the result of perturbations to the orbits of primordial binaries that brought the component stars closer together. In each case a CO-CO WD binary would have formed regardless of the perturbation but the orbital period would have been greater and merging would not have occurred.

At 4 Gyr one of the ONe–CO WD merger candidates remains in the cluster. It is not expected to merge for another 8 Gyr which is after the cluster will have completely dissolved. The other two ONe–CO WD binaries merged and formed neutron stars at ages of 63 and 75 Myr. The ONe–ONe WD binary formed after 61 Myr and the components were expected to merge shortly afterwards but in the interim the binary was ejected from the cluster. The five CO–CO WD binaries merged prior to 4 Gyr, the first after 110 Myr of evolution and the last at 2 666 Myr. Also formed during the simulation were ten double helium WD binaries with merging timescales less than 13 Gyr. Four of these escaped from the cluster prior to 4 Gyr. The other six remain in the cluster with periods of 0.04 to 0.08 d and three are experiencing steady mass transfer. In the BSE and `NBODY4` codes mass transfer from one WD to another occurs on a dynamical timescale if the mass ratio (donor/accretor) exceeds 0.628 and the outcome is coalescence of the WDs. If two He WDs merge it is assumed that the temperature produced is enough to ignite the triple-α reaction and that the nuclear energy released destroys the star. Four of the ten He–He WD binaries have mass ratios that satisfy this condition and two of them remain in the cluster at 4 Gyr. Iben (1990) discusses the possibility of subdwarf-O or B stars forming from merged He WDs which ignited helium at the base of the accretion layer. This alternative scenario of helium star formation had previously been mentioned by Webbink (1984).

6.3 Luminosity Functions

The luminosity function (LF) for the 616 single MS stars in Model 2 at 4 Gyr is shown in Figure 16. This is compared to the LF of the initial model (12 000 single MS stars) and also the LF at 4 Gyr for the model evolved with the population synthesis code. The latter distribution we call the non-dynamical LF and it contains 11 341 stars up to the MS turn-off at $V = 13$. So 659 stars have evolved off the MS by 4 Gyr. The primordial and non-dynamical MS LFs are identical for $V > 16$ and very similar up to $V = 13$ apart from some fluctuation owing to the evolution of near-turn-off stars. So the non-dynamical MS LF at 4 Gyr can be used to infer the IMF of the population. If the slope of the cluster MS LF matches that of the non-dynamical LF it would also retain an imprint of the IMF. However, we can see from Figure 16 that the two are far from being a good match. The cluster LF has been significantly flattened by the pref-

erential evaporation of low-mass stars from the cluster and by merging within binaries creating new MS stars near the turn-off.

In Figure 17 we split the cluster into five radial regions to examine the radial dependence of the MS LF slope and investigate whether there is any region which retains sufficient information about the IMF. There is a clear radial dependence with the central region containing many more massive stars than low-mass stars and the slope becomes flatter as we move outwards through the cluster. The normalized non-dynamical MS LF is compared to the cluster LF in each region and we can see that it is only in the outer regions that the slopes converge but, even then, the cluster LF is deficient in very low-mass stars and has an over-abundance of stars near the turn-off. Terlevich (1987) pointed out that in non-isolated clusters, heating by the galactic tide has the effect of making the velocity distribution isotropic and as such orbits ejected from the centre will tend to avoid returning there. This effect is in addition to mass segregation and helps in understanding the presence of massive MS stars in the outer regions. The LF for the five regions combined is also shown in Figure 17 and is essentially flat with a clear preference for massive MS stars compared to the non-dynamical (or field) distribution. Fan et al. (1996) show that the overall MS LF for M67 is quite flat and that the centre of the cluster is deficient in low-mass stars. They also found a radial dependence for the mass function slope. Bonatto & Bica (2003) confirm the tendency for massive stars in M67 to be more centrally concentrated and that the central regions of the cluster show a turnover in the cluster luminosity function at low masses. They find that the halo of the cluster is enriched in low-mass stars and their MS LF for the outer regions of M67 gives the best match to the expected LF slope for field stars (Kroupa, Tout & Gilmore 1993).

We have presented LFs of single MS stars as this is the ideal situation to deal with if one wants to make inferences about the IMF of the stellar population. Evolved stars such as giants complicate matters because they suffer mass loss and their luminosity evolution is not as well understood, and binary star evolution is obviously more uncertain than that of single stars. When dealing with observed data the goal is the same but the process is not as straightforward. Removing evolved stars from the LF by inspection of the CMD is not too difficult. Binaries with high mass-ratios can also be removed using the method of CMD inspection. However, low mass ratio binaries are problematic and will lead to contamination of the LF. In Figure 17 (sixth panel) we compare the slope of the LF for single MS stars to that of the same LF but with binaries with mass ratios less than 0.5 included as well. There are 532 single MS stars and 380 low–q binaries and the distributions have been normalized so that the slopes may be compared. We see that the inclusion of the low–q binaries does not affect the LF slope except at the low-mass end where binaries are biased towards high–q. Therefore, our model indicates that contamination of the MS LF by binaries is not necessarily a problem when using the shape of the distribution to infer the slope of the IMF.

7 DISCUSSION AND SUMMARY

A conclusion to draw from inspection of our two binary rich open cluster models is that in an open cluster, at least, one requires a substantial population of seed binaries capable of making BSs in order to explain the observed numbers of BSs. For Model 1 we used the birth period distribution suggested by Kroupa (1995b) to generate the orbital parameters of the 9 000 primordial binaries. Binary population synthesis told us to expect these binaries to produce just one BS after 4 Gyr of evolution and this would be via Case C mass transfer in a wide binary. After performing the N-body simulation we indeed found one BS in the model at 4 Gyr. For Model 2 we included 12 000 primordial binaries and chose the initial separation of each binary from a flat logarithmic distribution with an upper limit of 50 au. In this case we expected 25 BSs at 4 Gyr with 75 per cent being produced from Case A mass transfer in short-period systems. What we found after 4 Gyr of cluster evolution was 20 BSs with seven of these produced from non-perturbed primordial binaries. So the expected BSs were depleted while others were created. A major difference between the primordial binary setups of Models 1 and 2 is that the frequency of short-period binaries is much less in Model 1 and no BSs are expected to be produced from Case A mass-transfer in these binaries. The formation rate of non-primordial short-period binaries is very small in open cluster simulations and when it does occur it is generally as a result of a binary-binary encounter involving at least one existing short-period binary. Also, in the moderate density conditions of an open cluster we do not see BS formation from direct collisions of single stars while relatively wide primordial binaries may be destroyed in encounters with other stars before reaching a Case B or C mass-transfer stage. These factors explain the absence of BSs in Model 1 and tell us that the cluster environment on its own is not efficient at producing BSs. It is important to have a population of short-period binaries that either form BSs directly or become involved in dynamical encounters with other cluster stars and binaries and subsequently produce BSs. Our results indicate that period distributions such as Kroupa (1995b) and Duquennoy & Mayor (1991) that predict minimal BS formation from the standard Case A mass-transfer scenario are not suitable as initial conditions for open cluster binaries.

In Model 2 we observed formation pathways to explain the full variety of BSs found in M67, single BSs, super-BSs and binary BSs with a range of period–eccentricity combinations. At 4 Gyr we found that 50 per cent of the BSs are single and, of those in binaries, all but one has an eccentric orbit. This is in contrast to the binary population synthesis expectation for the primordial binaries of the model which gives a mix of 75 per cent single and only circular binaries. This tells us that dynamical encounters within the cluster environment play an important role in defining the nature of the BS population but perhaps not in boosting actual BS numbers. Less than half of the BSs were formed from primordial binaries that did not have their evolution altered in any way by dynamical encounters and the majority of these involved Case A mass transfer followed by coalescence to form a single BS. Other cases involved perturbations to the orbits of primordial binaries that induced mass transfer or, in some cases, a delay of mass-transfer after a primordial

binary became involved in a short-lived exchange encounter and emerged intact but with its orbital parameters altered. Mass transfer also led to BS formation in binaries created from exchange interactions. The alternative to BS formation via mass transfer is the collision of two MS stars at pericentre in a highly eccentric binary. This was observed to occur in primordial binaries with mildly eccentric orbits that had their eccentricity increased by perturbations received from nearby stars or binaries, often after becoming involved in a three- or four-body hierarchy. Exchange interaction also created highly eccentric binaries in which the component stars eventually collided to form a BS. Mapelli et al. (2004) showed that the radial distribution of BSs observed in the globular cluster 47 Tucanae is best explained by formation from primordial binaries (mass-transfer scenario) in the outer regions of the cluster and a mixture of exchange-induced collisions and primordial binary evolution in the core. So even though the stellar environment is very different in the core of 47 Tucanae than in M67 it seems that a mixture of BS formation scenarios is favourable in both. Davies, Piotto & De Angeli (2004) demonstrated that exchange interactions can be detrimental to BS formation via primordial binaries in massive globular clusters. They consider that exchanges produce binaries with increasingly more-massive components and this could lead to binaries that would have created a BS to be observed in a globular cluster now being replaced by binaries that form BSs much earlier. Their experiments showed that an average number of encounters per binary of about 5 to 10 was beneficial for BS production and that anything in excess of this would seriously hamper the BS formation rate. This result is tuned to the age and turn-off mass of globular clusters and is also dependent on the distribution of binary separations but we note that in our open cluster simulations only a few per cent of the binaries were involved in multiple exchange encounters.

Because a significant fraction of the BSs in our model are influenced in some way by the formation of triple and quadruple subsystems it would seem prudent to consider including a primordial population of these. Especially as triple and higher-order systems are observed in young open clusters (Schertl et al. 2003) and the field (Tokovinin 1997). Sandquist (2004) mentions nine possible triple systems in M67. Also, van den Berg et al. (2001) identified the BS S1082 in M67 (classified as single by Milone & Latham 1992) with a spectroscopic close binary and based on X-ray emission it is now thought to be a triple system containing an RS CVn star with the BS as the outer component (van den Berg et al. 2004). Our M67 model at 4 Gyr contains 20 hierarchical triples and there are 20 to 30 stable triples in the Model 2 simulation at any time. None of the BSs in the model at 4 Gyr are in triple systems although one BS-binary is loosely bound to another binary with an orbital separation of 5×10^4 au. There are instances of triples containing a BS at other times, primarily as a result of a BS forming in an eccentric binary collision within a four-body or higher order system and remaining bound to other members of the system. These are not generally long-lived. Short-lived triple systems are also found to be responsible for inducing an eccentricity in the orbits of previously circular BS binaries. This is the Kozai effect (Kozai 1962) produced by a cyclic relation between the inner eccentricity and the orbital inclination and which is modelled in `NBODY4` (Aarseth 2003). One of the RS CVn binaries in Model 2 at 4 Gyr (#1568) is the inner binary of a triple system with a $1.3 M_\odot$ MS star and an outer period of about 1 000 d. The capability to include primordial triple and quadruple systems has recently been added to `NBODY4` and we plan to utilize this in future simulations.

Mathieu et al. (2003) report the finding of two spectroscopic binaries in M67 with a position in the CMD about 1 mag below the subgiant branch. They are high-probability proper-motion members and have also been confirmed as X-ray sources (van den Berg, Verbunt & Mathieu 1999). Based on their CMD position the primaries of these binaries are termed sub-subgiants and it has been postulated that they are the products of stellar encounters on non-standard evolutionary tracks (Mathieu et al. 2003). One binary is circular with a period of 2.82 d and the other has an eccentricity of 0.21 and a period of 18.4 d. The eccentric binary is in the core of M67 and shows high reddening which implies a subgiant with extinction (Mathieu et al. 2003). The star lying below the subgiant branch in our M67 model was formed in a CE event that saw $0.29 M_\odot$ of material ejected from the star when the cores merged. Extinction from this material was not considered when calculating the CMD position of the star but this possibility and its position below the subgiant branch make it a candidate sub-subgiant explanation. However, to explain the binary nature the star would need to have been a member of a triple system in which the merged star remained bound to the third component. This is not an unrealistic scenario and the inclusion of primordial triples would make it more likely.

The M67 model we have presented here is a marked improvement on the model previously reported in Hurley et al. (2001). A major reason for this is in the construction of the models. The current model is the result of an N-body simulation that was evolved from zero-age whereas the Hurley et al. (2001) N-body model started at 2.5 Gyr. Also Hurley et al. (2001) subjected their model to an unusually strong tidal field in an attempt to produce a cluster that contained the observed mass of M67 within a tidal radius of 10 pc. More recent observations suggest that the tidal radius of M67 is actually greater than this. To achieve our preferred M67 model (Model 2 at 4 Gyr) we did make an alteration to the tidal field. Model 2 placed the cluster on an orbit at 8 kpc from the Galactic centre as opposed to 8.5 kpc for the standard orbit used in Model 1. This is well within the bounds allowed by the actual orbit of M67 and an orbital speed of $220\,\mathrm{km\,s^{-1}}$ was used for both Models 1 and 2. Hurley et al. (2001) used $350\,\mathrm{km\,s^{-1}}$. So the modification of the tidal field for Model 2 is nowhere near as extreme as for the Hurley et al. (2001) model. In fact, according to Baumgardt (1998) it is the tidal radius at perigalacticon that determines the cluster dissolution timescale and considering that M67 has a perigalacticon of 6.8 kpc we could have chosen an even stronger tidal field for Model 2, and thus started with a greater number of stars and binaries.

Results are also better for our new M67 model because half of the BSs are found in binaries compared to only one out of 22 found by Hurley et al. (2001). The raw numbers of BSs are similar but the Hurley et al. (2001) model actually did better at creating BSs by dynamical means – they expected only half as many BSs as their model produced

whereas our model actually produces slightly less than expected. Comparison of the two models is not straightforward because different distributions were used for the primordial binary separations and other factors such as the tidal field used by Hurley et al. (2001) significantly alter the evolution of the cluster. Also, the semi-direct nature of the Hurley et al. (2001) model, which started with 5 000 single stars and 5 000 binaries at an age of 2.5 Gyr, complicates direct comparison. Our model with initially 12 000 single stars and 12 000 binaries actually contained 4 322 single stars and 4 859 binaries after 2.5 Gyr of evolution so the numbers are comparable at this stage. However, in an attempt to compensate for skipping 2.5 Gyr of N-body evolution Hurley et al. (2001) selected their primordial binaries using a mass function biased towards higher masses and then evolved these to an age of 2.5 Gyr with the BSE code. Comparison of this population with our 4 859 binaries at 2.5 Gyr shows that the Hurley et al. (2001) model has a higher proportion of binaries with a combined mass in excess of the cluster turn-off mass at 4 Gyr. The semi-direct model also evolved at higher central density ($\rho_c > 1\,000\,\mathrm{stars\,pc^{-3}}$ for the majority of the simulation) and with a smaller half-mass radius. This would explain the increased incidence of dynamical BS formation.

It is reassuring that the structure of our M67 model provides a good match to the observed structure of M67. The half-mass radius, the tidal radius and the mass of the model and cluster are all in agreement. The surface density profile of the model is also able to reproduce the observed M67 profile, except in the core where the model has too many stars. We have constructed a surface brightness profile for the model using the same software as used for treating observed data and found that it is very well fitted by an Elson, Fall & Freeman (1987) distribution. This distribution was determined from young and intermediate age clusters in the Large Magellanic Clouds which do not show the same degree of tidal truncation as the old globular clusters of our Galaxy to which the King (1962) models were fitted. Differences between the Elson, Fall & Freeman (1987) model and the King (1962) model are only apparent near the tidal radius of a cluster. The luminosity functions for MS stars in various spatial regions of our M67 model also give good agreement with the observed behaviour. Our M67 model has done a very good job of simulating the blue straggler and RS CVn stars observed in M67. So the model places strong constraints on the parameters of the primordial binary population in this cluster. Also, by matching the properties of populations for which observations are likely to be complete (BSs and RS CVn stars), we can use the model to make predictions about the completeness of other populations (e.g. white dwarfs and BY Draconis stars).

The process of tailoring a simulation to the parameters of a particular cluster and taking the time to compare the real and model data in a consistent manner has certainly proved fruitful. An effort along these lines was made previously by Portegies Zwart et al. (2001) who looked at young open clusters such as the Hyades using models of $N \simeq 3\,000$, whereas we have focussed on old clusters where the interaction between dynamical, stellar and binary evolution is more pronounced. We look forward to taking this approach with other rich open clusters of various ages, such as NGC 2099 (Kalirai et al. 2001) and NGC 188 (Stetson, McClure & VandenBerg 2004), in order to further understanding the initial conditions, dynamical history and stellar populations of these objects. It can then be taken into the globular cluster regime when the petaflops speed GRAPE-DR (Makino et al. 2003) eventually becomes available. We also urge those working on observations of star clusters to take full advantage of dynamical models when interpreting data.

ACKNOWLEDGMENTS

We thank Charles Bonatto for providing us with M67 data and allowing this to be used in the paper. Thanks to Dougal Mackey for providing his surface brightness profile software as well as advice on how to use it. We are grateful to Maureen van den Berg for clarifying the M67 Chandra data and making useful comments on the manuscript. JRH thanks the Australian Research Council for a Fellowship and is grateful to the Institute of Astronomy, Cambridge for hosting a visit during this work. CAT thanks Churchill College for a Fellowship. We acknowledge the generous support of the Cordelia Corporation and that of Edward Norton which has enabled AMNH to purchase GRAPE-6 boards and supporting hardware.

REFERENCES

Aarseth S. J., 1966, in Kontopoulos G., ed, Proc, IAU Symp. 25, The Theory of Orbits in the Solar System and in Stellar System. Academic Press, London, p. 141

Aarseth S. J., 1996, in Milone E., Mermilliod J.-C., eds, ASP Conf. Series, Vol. 90, The Origins, Evolution, and Destinies of Binary Stars in Clusters. ASP, San Francisco, p. 423

Aarseth S. J.,1999, PASP, 111, 1333

Aarseth S.J., 2003, Gravitational N-body Simulations: Tools and Algorithms (Cambridge Monographs on Mathematical Physics). Cambridge University Press, Cambridge

Aarseth S., Hénon M., Wielen R., 1974, A&A, 37, 183

Abt H.A., 1983, ARA&A, 21, 343

Ahumada J., Lapasset E., 1995, A&AS, 109, 375

Baumgardt H., 1998, A&A, 330, 480

Baumgardt H., 2001, MNRAS, 325, 1323

Baumgardt H., Makino J., 2003, MNRAS, 340, 227

Belloni T., Verbunt F., Mathieu R.D., 1998, A&A, 339, 431

Bergeron P., Wesemael F., Beauchamp A., 1995, PASP, 107, 1047

Bonatto Ch., Bica E., 2003, A&A, 405, 525

Bonatto Ch., Bica E., 2005, astro-ph/0503589

Carraro G., Chiosi C., 1994, A&A, 288, 751

Casertano S., Hut P., 1985, ApJ, 298, 80

Chernoff D.F., Weinberg M.D., 1990, ApJ, 351, 121

Davies M.B., Piotto G., De Angeli F., 2004, MNRAS, 349, 129

Djorgovski S., 1988, in Proc. IAU Symp. 126, The Harlow-Shapley Symposium on Globular Cluster Systems in Galaxies. Kluwer, Dordrecht, p. 333

Duquennoy A., Mayor M., 1991, A&A, 248, 485

Eggleton P.P., Fitchett M., Tout C.A., 1989, ApJ, 347, 998

Elson R.A.W., Fall S.M., Freeman K.C., 1987, ApJ, 323, 54

Fan X., et al., 1996, AJ, 112, 628

Giersz M., Heggie D.C., 1994, MNRAS, 268, 257

Girard T.M., Grundy W.M., López C.E., van Altena W.F., 1989, AJ, 98, 227

Grindlay J.E., Heinke C., Edmonds P.D., Murray S.S., 2001, Science, 292, 2290

Hall D.S., 1976, in Fitch W.S., ed, Proc. IAU Colloq. 29, Multiple Periodic Variable Stars. Reidel, Dordrecht, p. 287

Heggie D.C., 1975, MNRAS, 173, 729

Heggie D.C., Hut P., McMillan S.L.W., 1996, ApJ, 467, 359

Hobbs L.M., Thorburn J.A., 1991, AJ, 102, 1070

Hurley J. R., Shara M.M., 2003, ApJ, 589, 179

Hurley J. R., Pols O.R., Tout C. A., 2000, MNRAS, 315, 543

Hurley J. R., Tout C. A., Aarseth S. J., Pols,O.R., 2001, MNRAS, 323, 630

Hurley J. R., Tout C. A., Aarseth S. J., Pols,O.R., 2004, MNRAS, 355, 1207

Hurley J. R., Tout C. A., Pols,O.R., 2002, MNRAS, 329, 897

Iben I.Jr., 1990, ApJ, 353, 215

Janes K.A., Phelps R.L., 1994, AJ, 108, 1773

Kafka S., Gibbs D.G.II., Henden A.A., Honeycutt R.K., 2004, AJ, 127, 1622

Kalirai J. S., et al., 2001, AJ, 122, 266

Kalirai J. S., Fahlman G.G., Richer H.B., Ventura P., 2003, AJ, 126, 1402

King I.R., 1962, AJ, 67, 471

King I.R., 1966, AJ, 71, 64

Kippenhahn R., Wiegert A., Hoffmeister R., 1967, in Alder B., Fernbach S., Rotenburg M., eds, Methods in Computational Physics, Vol. 7, Astrophysics, New York, p. 129

Kochanel C.S., 1992, ApJ, 385, 604

Kozai Y., 1962, AJ, 67, 591

Kroupa P., 1995a, MNRAS, 277, 1491

Kroupa P., 1995b, MNRAS, 277, 1507

Kroupa P., Aarseth S., Hurley J., 2001, MNRAS, 321, 699

Kroupa P., Tout C. A., Gilmore G., 1991, MNRAS, 251, 293

Kroupa P., Tout C. A., Gilmore G., 1993, MNRAS, 262, 545

Kurucz R.L., 1992, in Barbuy B., Renzini A., eds, Proc. IAU Symp. 149, The Stellar Populations of Galaxies. Kluwer, Dordrecht, p. 225

Lang K.R., 1992, Astrophysical Data. Springer-Verlag, Berlin

Latham D.W., Milone A.A.E., 1996, in Milone E.F., Mermilliod J.-C., eds, ASP Conf. Series, Vol. 90, The Origins, Evolution, and Destinies of Binary Stars in Clusters. ASP, San Francisco, p. 385

Leonard P.J.T., 1996, ApJ, 470, 521

Lombardi J.C., Rasio F.A., Shapiro S.L., 1996, ApJ, 468, 797

Lombardi J.C., Thrall A.P., Deneva J.S., Fleming S.W., Grabowski P.E., 2003, MNRAS, 345, 762

Mackey A.D., Gilmore G.F., 2003, MNRAS, 338, 85

Makino J., 1991, ApJ, 369, 200

Makino J., 2002, in Shara M.M., ed, ASP Conference Series 263, Stellar Collisions, Mergers and their Consequences. ASP, San Francisco, p. 389

Makino J., Taiji M., 1998, Scientific Simulations with Special-Purpose Computers – the GRAPE Systems. Wiley, New York

Makino J., Fukushige T., Koga M., Namura K., 2003, PASJ, 55, 1163

Mathieu R.D., van den Berg M., Torres G., Latham D., Verbunt F., Stassun K., 2003, AJ, 125, 246

Mapelli M., Sigurdsson S., Colpi M., Ferraro F.R., Possenti A., Rood R.T., Sills A., Beccari G., 2004, ApJ, 605, L29

Mardling R.A., Aarseth S.J., 2001, MNRAS, 321, 398

McMillan S.L.W., 1986, in Hut P., McMillan S.L.W., eds, The Use of Supercomputers in Stellar Dynamics. Springer-Verlag, Berlin, p. 156

Mikkola S., Aarseth S.J., 1993, Celest. Mech. Dyn. Astron., 57, 439

Mikkola S., Aarseth S.J., 1998, New Astronomy, 3, 309

Milone A.A.E., Latham D.W., 1992, in Kondo, Y., Sisteró R.F., Polidan R.S., eds, Proc. IAU Symp. 151, Evolutionary Processes in Interacting Binary Stars. Kluwer, Dordrecht, p. 475

Montgomery K.A., Marschall L.A., Janes K.A., 1993, AJ, 106, 181

Nomoto K., Kondo Y., 1991, ApJ, 367, L19

Piotto G., et al., 2002, A&A, 391, 945

Plummer H.C., 1911, MNRAS, 71, 460

Pols O.R., Karakas A.I., Lattanzio J.C., Tout C.A., 2003, ASPC, 303, 290

Pols O.R., Schröder K.-P., Hurley J.R., Tout C.A., Eggleton P.P., 1998, MNRAS, 298, 525
Pooley D., et al., 2003, ApJ, 591, L131
Portegies Zwart S.F., McMillan S.L.W., Hut P., Makino J., 2001, MNRAS, 321, 199
Portegies Zwart S.F., Hut P., McMillan S.L.W., Makino J., 2004, MNRAS, 351, 473
Press W.H., Teukolsky S.A., 1977, ApJ, 213, 183
Preston G.W., Sneden C., 2000, AJ, 120, 1014
Randich S., 1997, MmSAI, 68, 971
Richer H.B., Fahlman G.G., Rosvick J., Ibata R., 1998, ApJ, 116, L91
Richer H.B., et al., 2004, AJ, 127, 2771
Saio H., Nomot K., 1998, ApJ, 500, 388
Sandquist E.L., 2004, MNRAS, 347, 101
Sandquist E.L., Shetrone M.D., 2003, AJ, 125, 2173
Schertl D., Balega Y.Y., Preibisch Th., Weigelt G., 2003, A&A, 402, 267
Shara M.M., Hurley J.R., 2002, ApJ, 571, 830
Sills A., Faber J.A., Lombardi J.C., Rasio F.A., Warren A.R., 2001, ApJ, 548, 323
Sills A., et al., 2003, New Astronomy, 8, 605
Stetson P.B., McClure R.D., VandenBerg D.A., 2004, PASP, 116, 1012
Tautvaišienė G., Edvardsson B., Tuominen I., Ilyin, I., 2000, A&A, 360, 499
Terlevich E., 1987, MNRAS, 224, 193
Tokovinin A.A., 1997, A&AS, 124, 75
van Albada T.S., 1968, Bull. Astron. Inst. Neth., 19, 479
VandenBerg D.A., Stetson P.B., 2004, PASP, 116, 997
van den Berg M., Verbunt F., Mathieu R.D., 1999, A&A, 347, 866
van den Berg M., Orosz J., Verbunt F., Stassun K., 2001, A&A, 375, 375
van den Berg M., Tagliaferri G., Belloni T., Verbunt F., 2004, A&A, 418, 509
Vesperini E., 1997, MNRAS, 287, 915
von Hoerner S., 1960, Z. Astrophys., 50, 184
Walter F.M., 1982, ApJ, 253, 745
Webbink R.F.,1984, ApJ, 277, 355
Webbink R.F.,1998, in Mikolajewska J., Friedjung M., Kenyon S.J., Viotto R., eds, Proc. IAU Colloq. 103, The Symbiotic Phenomenon. Kluwer, Dordrecht, p. 311
Wilkinson M.I., Hurley J.R., Mackey A.D., Gilmore G.F., Tout C.A., 2003, MNRAS, 343, 1025
Yungelson L., Livio M., 2000, ApJ, 528, 108

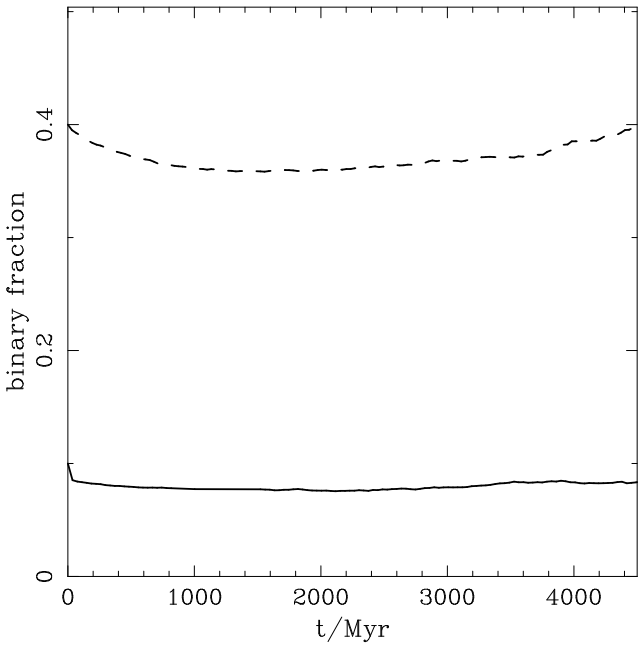

Figure 1. Evolution of binary fraction with age for an N-body cluster model starting with 18 000 stars and 2 000 binaries (Shara & Hurley 2002: solid line). Also shown is a model that started with 12 000 stars and 8 000 binaries (Hurley & Shara 2003: dashed line).

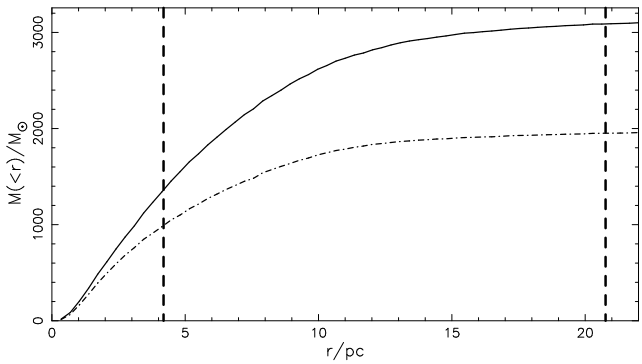

Figure 2. The mass profile of Model 1 at 4 Gyr. The solid line represents the total cluster mass and the dashed-dot line is the luminous mass. Dashed vertical lines show the tidal radius (20.8 pc) and the half-mass radius for the luminous mass (4.2 pc).

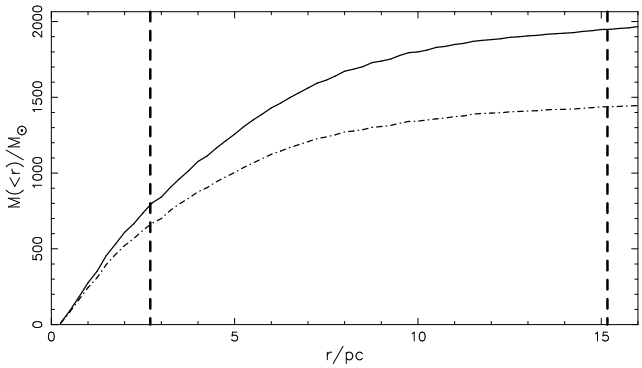

Figure 3. The mass profile of Model 2 at 4 Gyr. The solid line represents the total cluster mass and the dashed-dot line corresponds to the luminous mass. Dashed vertical lines show the tidal radius (15.2 pc) and the half-mass radius for the luminous mass (2.7 pc).

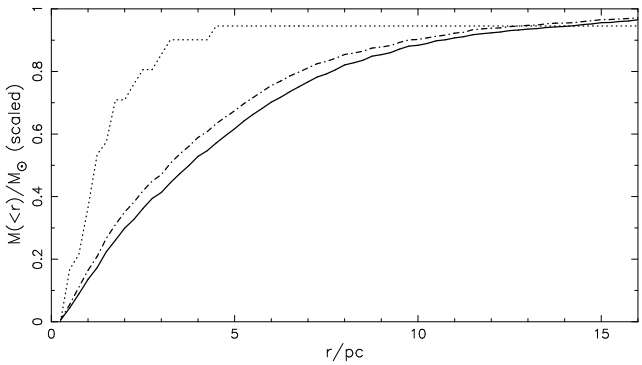

Figure 4. Mass profiles for Model 2 at 4 Gyr scaled by the total mass involved in constructing the profile, all stars (solid line), luminous mass (dashed-dot line) and the blue straggler mass (dotted line).

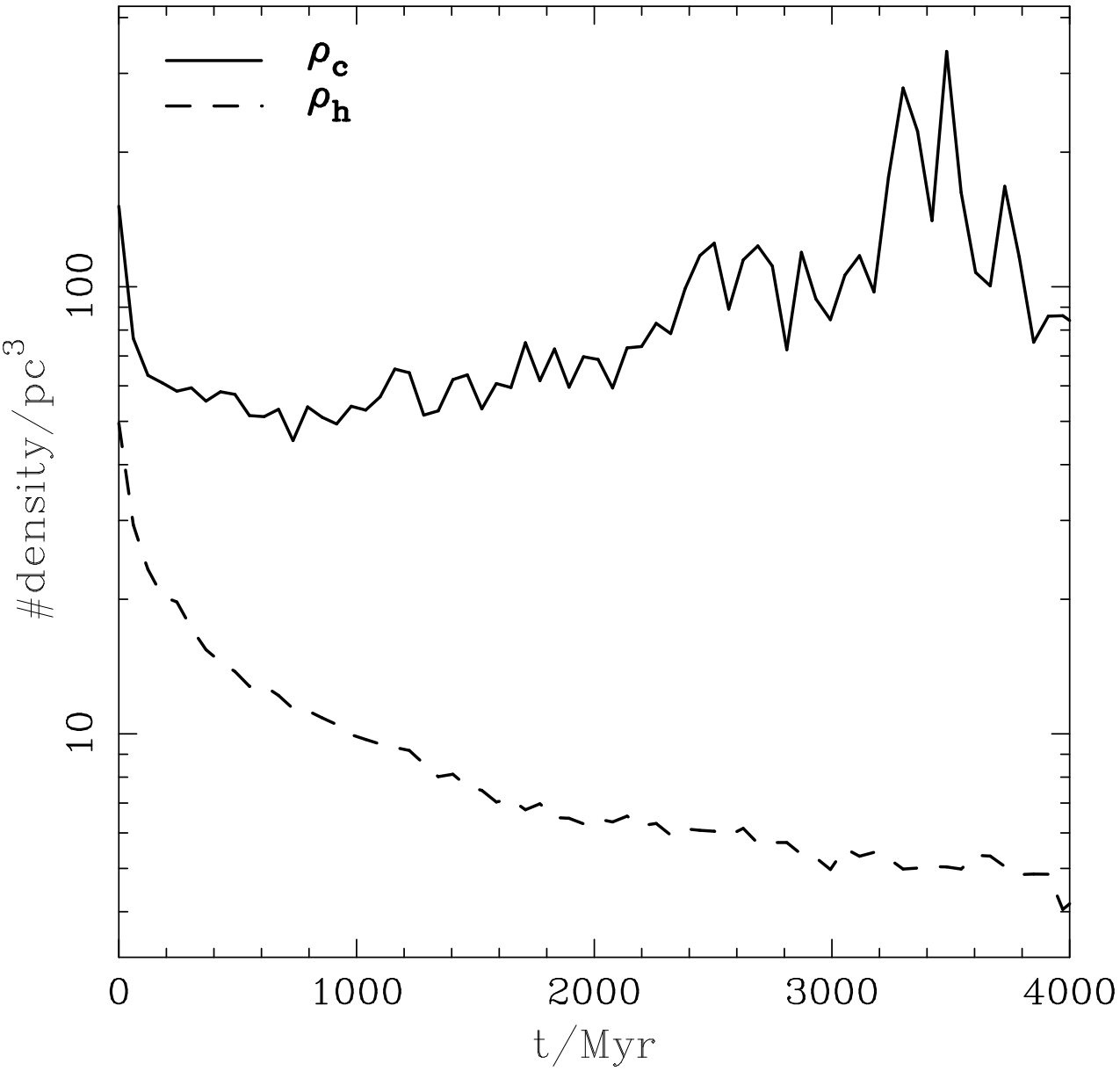

Figure 5. Evolution of the number density of stars within the core (solid line) and the half-mass radius (dashed line) for Model 2.

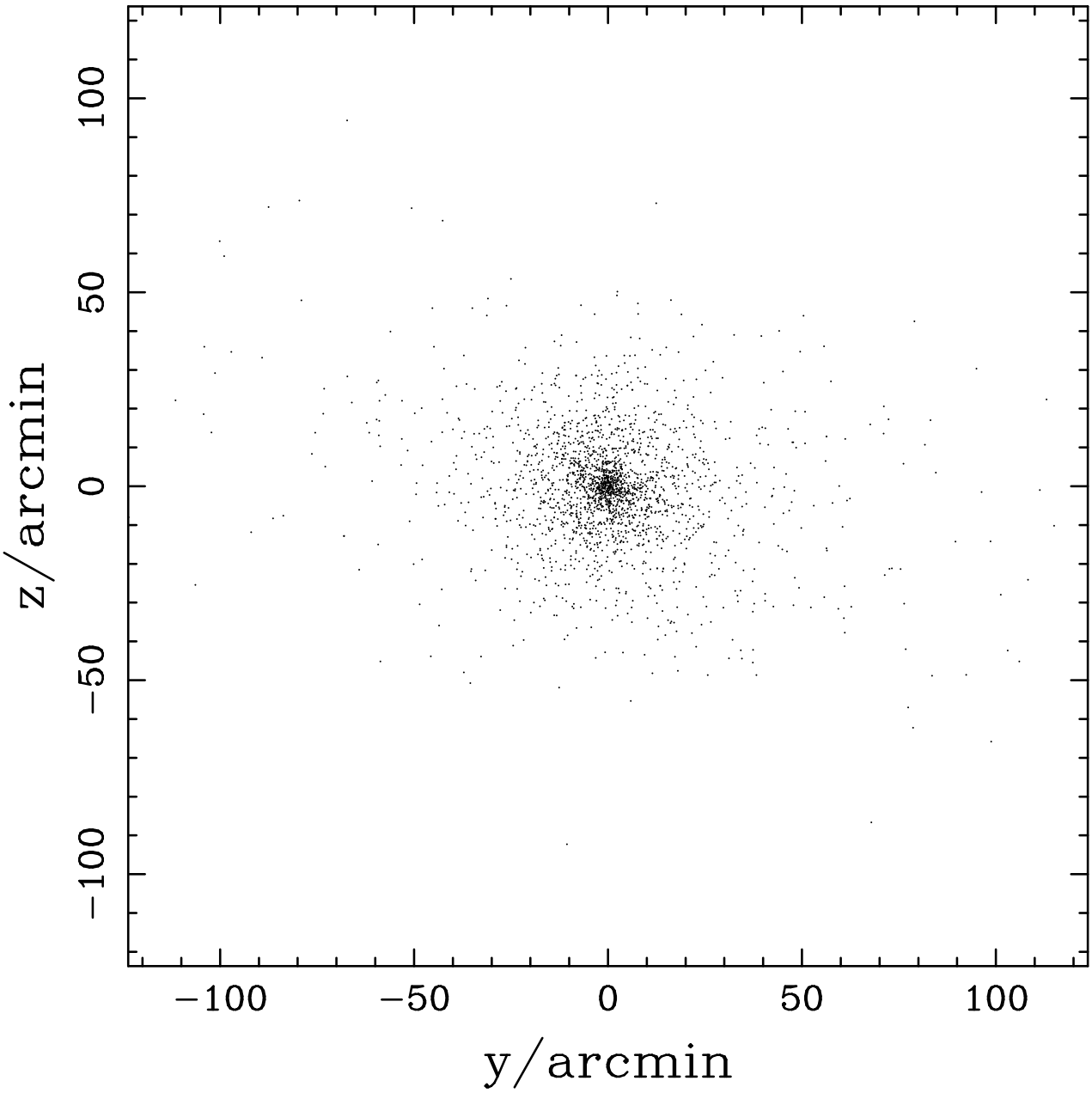

Figure 6. Model 2 at 4 Gyr shown in the observed plane (the yz- or transformed YZ-plane).

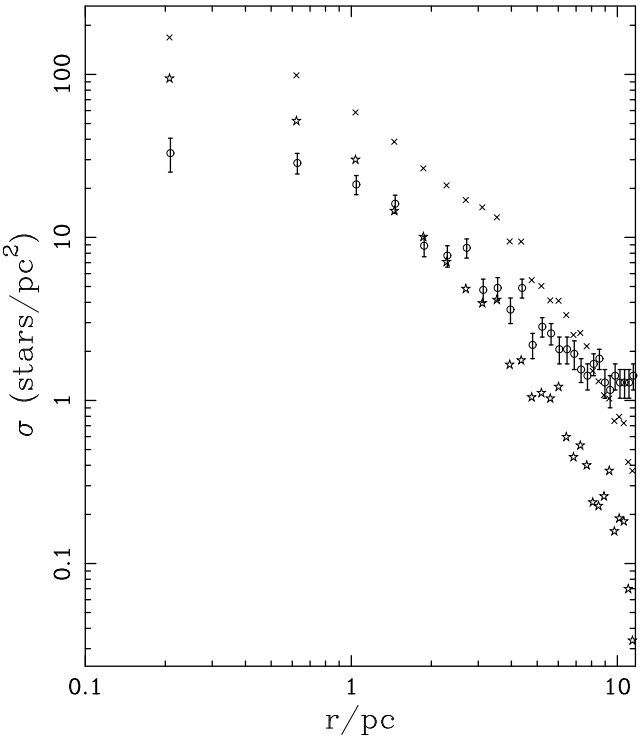

Figure 7. Surface density profile of M67 from 2MASS data provided by Bonatto (private communication: open circles). Profiles from the model for all stars (× symbols) and for only luminous stars with mass greater than $0.8M_{\odot}$ (open star symbols) are also shown. The distributions have not been normalized. 1σ error bars have been included for the observed profile but for the sake of clarity we have not included error bars for the model points although the errors will be of comparable magnitude.

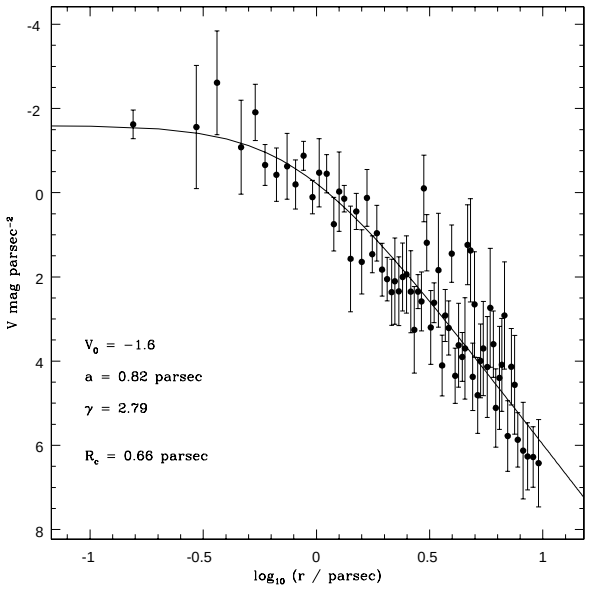

Figure 8. Surface brightness profile for Model 2 at 4 Gyr (solid data points) constructed using software provided by Mackey & Gilmore (2003). The projection is along the Y-axis. Error bars are calculated according to the method outlined by Djorgovski (1988, in IAU Symp. 126, p333) where a given annulus is split into eight sectors of equal area. The internal error for the annulus is the standard deviation of the surface brightness values for the eight sectors. A fit to the data of an Elson, Fall & Freeman (1987) model (solid line) gives a core radius of 0.66 pc. This is a three-parameter model $V(r) = V_0(1 + r^2/a^2)^{-\gamma/2}$ where V_0 is the central surface brightness and a is related to the core radius by $r_{\rm c} = a(2^{2/\gamma} - 1)^{1/2}$. The χ^2 error of the fit is 1.05 which represents the sum of the squares of the differences between the data and model points in each bin weighted by the error for that bin.

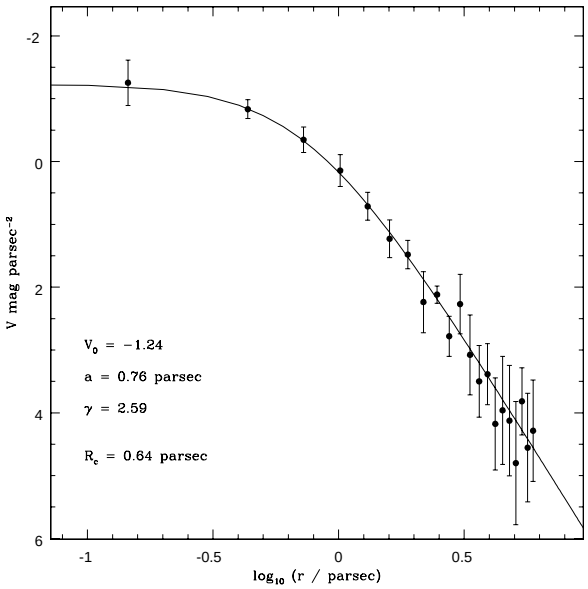

Figure 9. Same as Figure 8 but restricted to stars in the range $12 < V < 17$. The main-sequence turn-off is at $V \simeq 13$ (corresponding to a mass of $1.32M_{\odot}$) so the range covers one magnitude above the turn-off, approximately half-way up the giant branch, and four magnitudes below the turn-off, down to a mass of $0.75M_{\odot}$. The surface density profile fit has a scaled χ^2 error of 0.25 and gives a core radius of 0.64 pc.

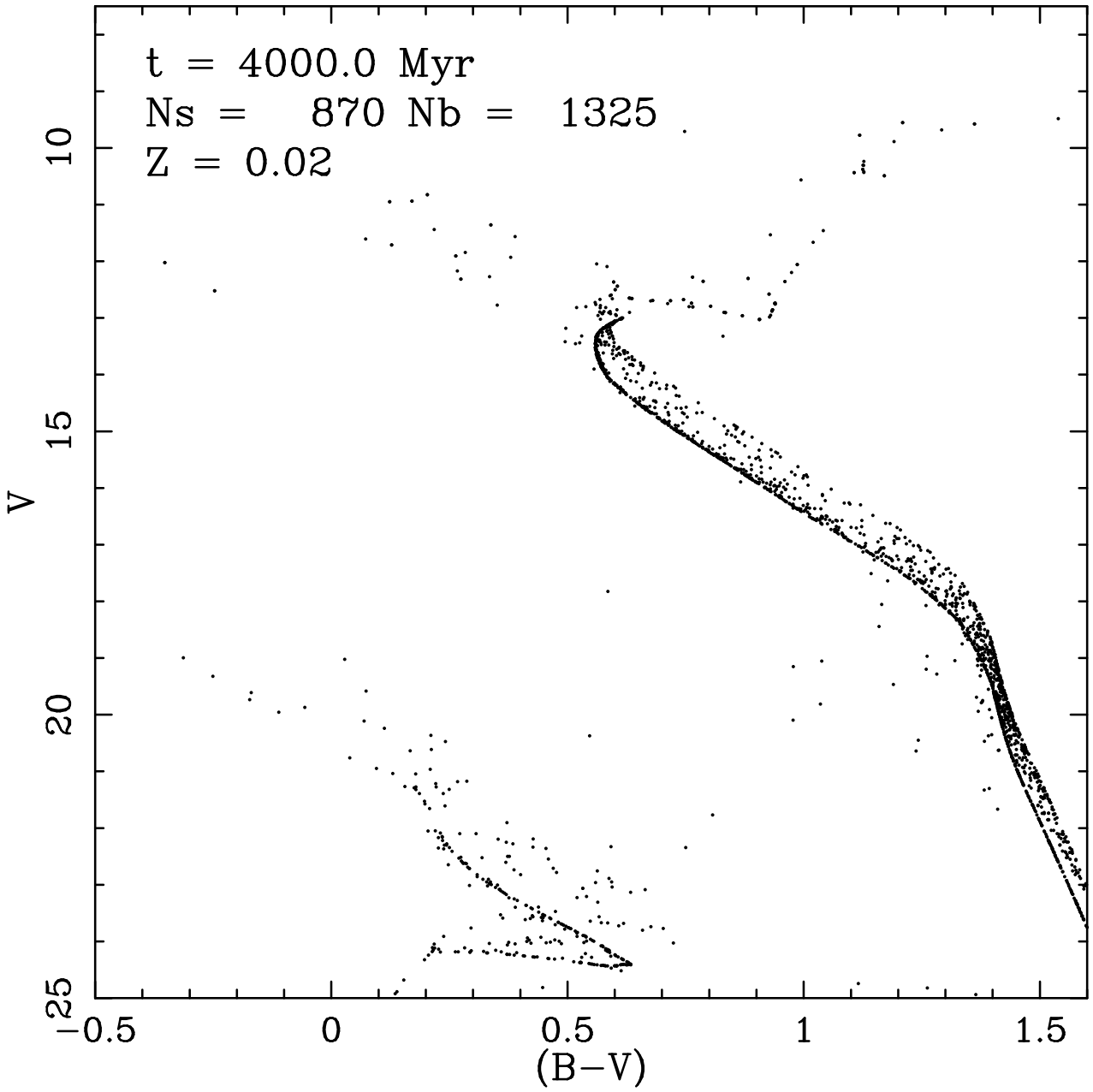

Figure 10. Cluster colour-magnitude diagram at 4.0 Gyr. Note that all binaries are assumed to be unresolved. To convert the luminosities and effective temperatures to magnitude and colour we have used the bolometric corrections given by Kurucz (1992) and, in the case of WDs, Bergeron, Wesemael & Beauchamp (1995). A distance modulus of 9.7 (Hurley et al. 2001) has been assumed to place the simulated cluster at the distance of M67.

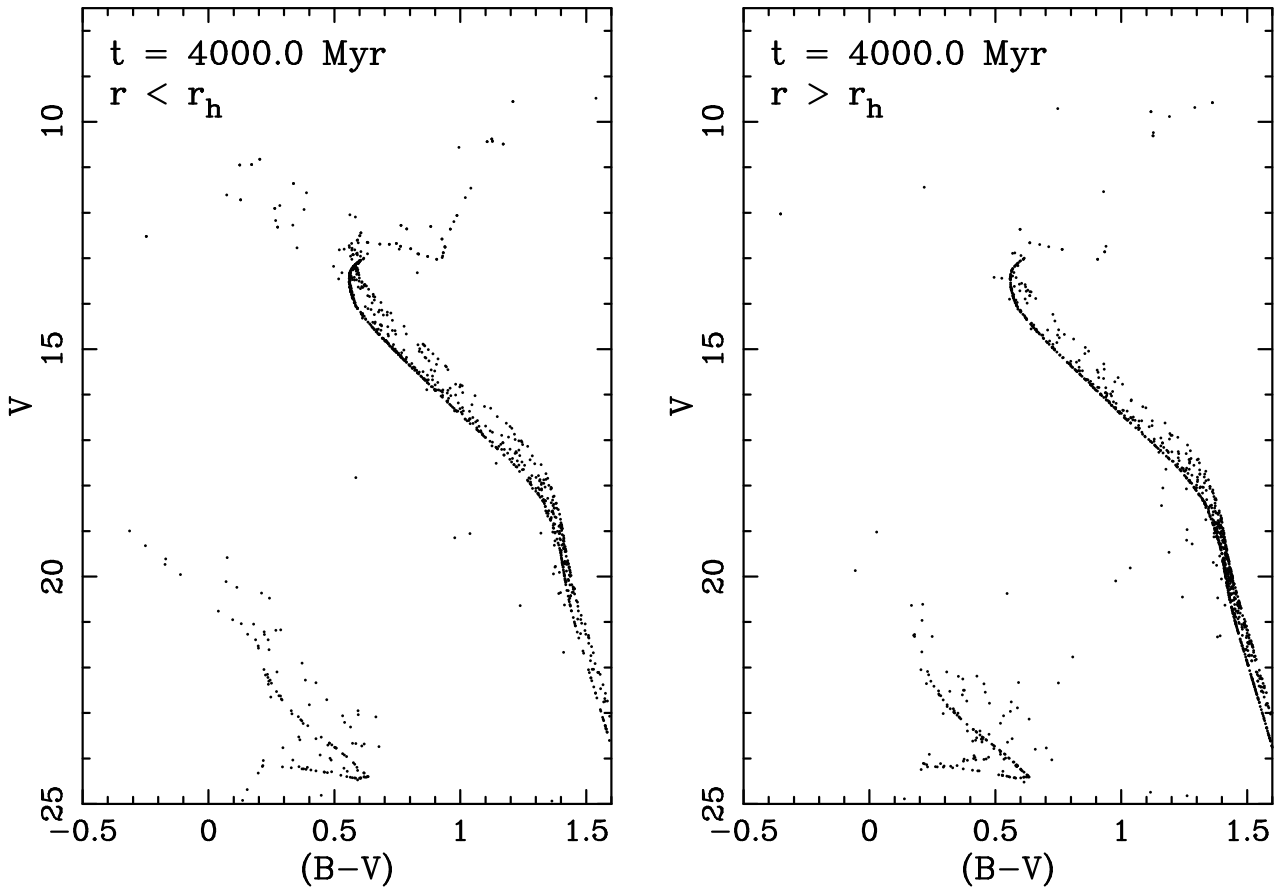

Figure 11. As for Figure 10 but for stars within the half-mass radius (3.8 pc) of the cluster (left panel) and exterior to the half-mass radius (right panel).

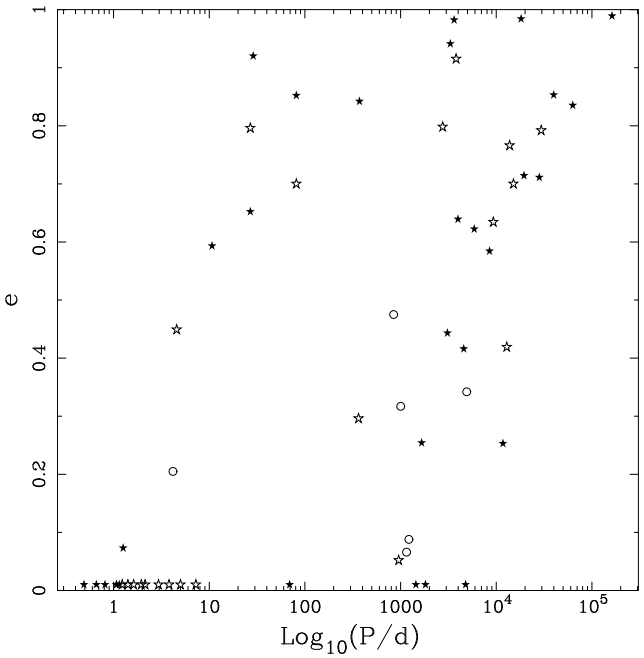

Figure 12. Distribution of periods and eccentricities for binaries found to contain a BS that were present in the M67 simulation (Model 2) at an age of 2 Gyr or later. The solid stars represent the orbital periods at the time of formation, when one of the stars became a BS or when a BS was exchanged in to a new binary (31 points). If the orbital parameters of any of these binaries subsequently experienced a significant change ($\Delta e > 0.05$ and/or $\Delta \log P/\mathrm{d} > 0.1$), owing to binary evolution or a perturbation, this is represented by an open star (21 points). Orbital parameters for the six BS binaries known to reside in M67 are denoted by open circles.

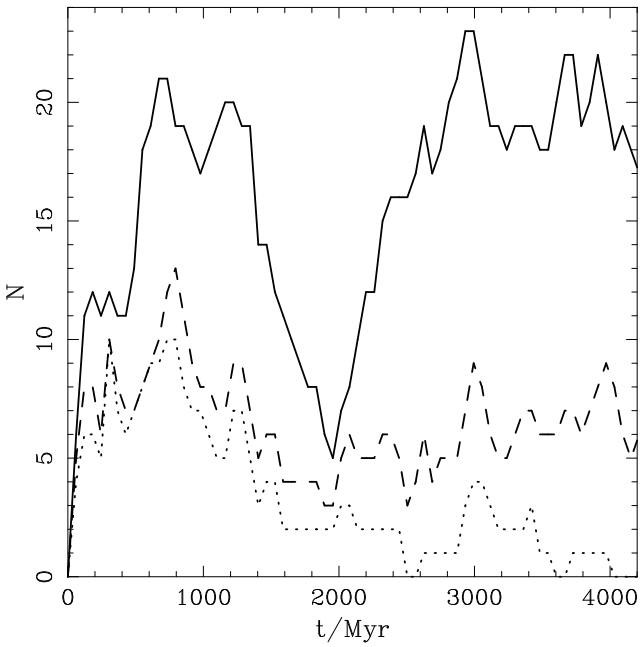

Figure 13. Number of BSs (solid line), BS-binaries (dashed line) and circular BS-binaries with $P < 100\,\mathrm{d}$ (dotted line) during the M67 simulation (Model 2).

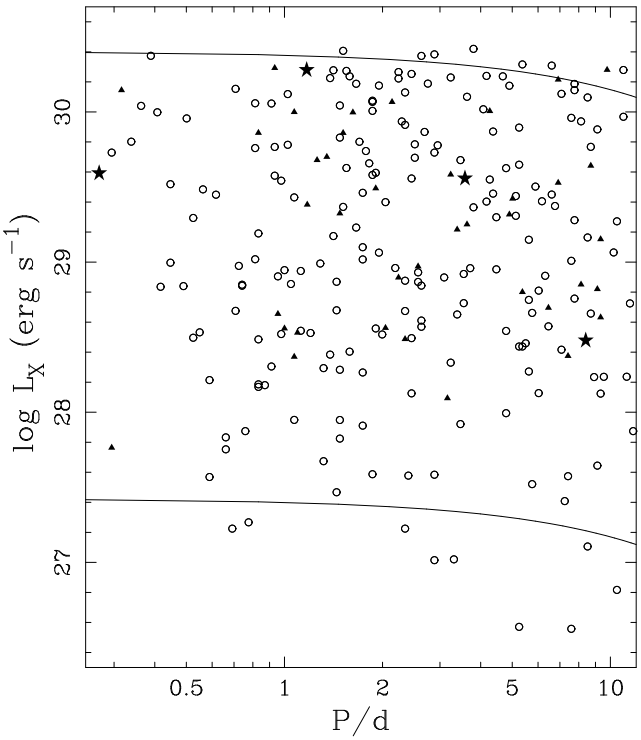

Figure 14. X-ray luminosity as a function of orbital period for MS-MS binaries with a primary mass of $1.0 M_\odot$ or less (open circles) and for MS-WD binaries (solid triangles). The upper solid line shows the X-ray luminosity for a $1.0 M_\odot$ MS star at an age of 4 Gyr calculated from Equation 2 as a function of orbital period, assuming that the star is in a binary of that period and experiencing synchronous rotation. The lower solid line is for a $0.1 M_\odot$ MS star. We also include data points (solid stars) for the possible BY Draconis systems identified by van den Berg et al. (2004) for which an orbital period is known (L_X values for these systems supplied by M. van den Berg, private communication).

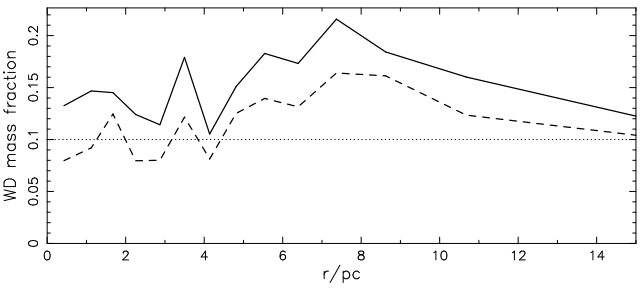

Figure 15. Mass fraction of white dwarfs in Model 2 at 4 Gyr as a function of radius. The radial bins are chosen so that 150 stars are sampled in each bin. Results for all WDs (solid line) and for only single WDs and double WDs (dashed line) are shown. The dotted line at $f_{\mathrm{WD}} = 0.1$ is the value expected from isolated population synthesis of the initial stars.

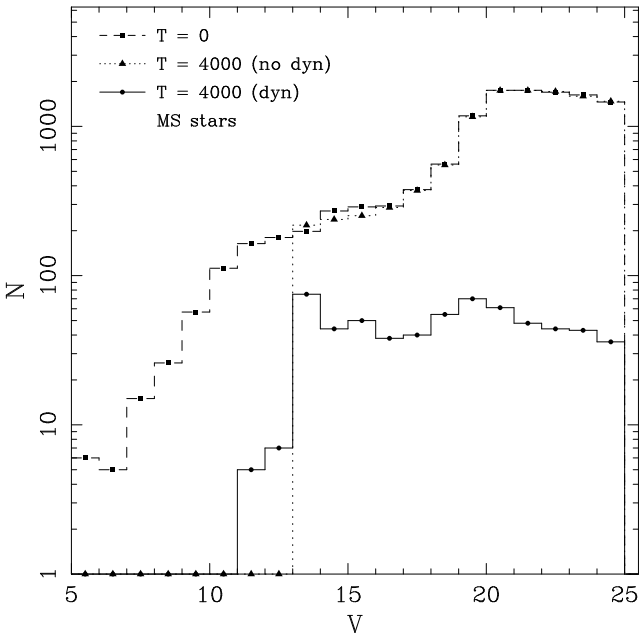

Figure 16. Luminosity function of single main-sequence stars in Model 2 at time zero (dashed line, 12 000 stars) and at 4 Gyr (solid line, 616 stars). Also shown is the luminosity function for the initial stars evolved to 4 Gyr with the population synthesis code (dotted line, 11 341 stars). The histograms are not normalized.

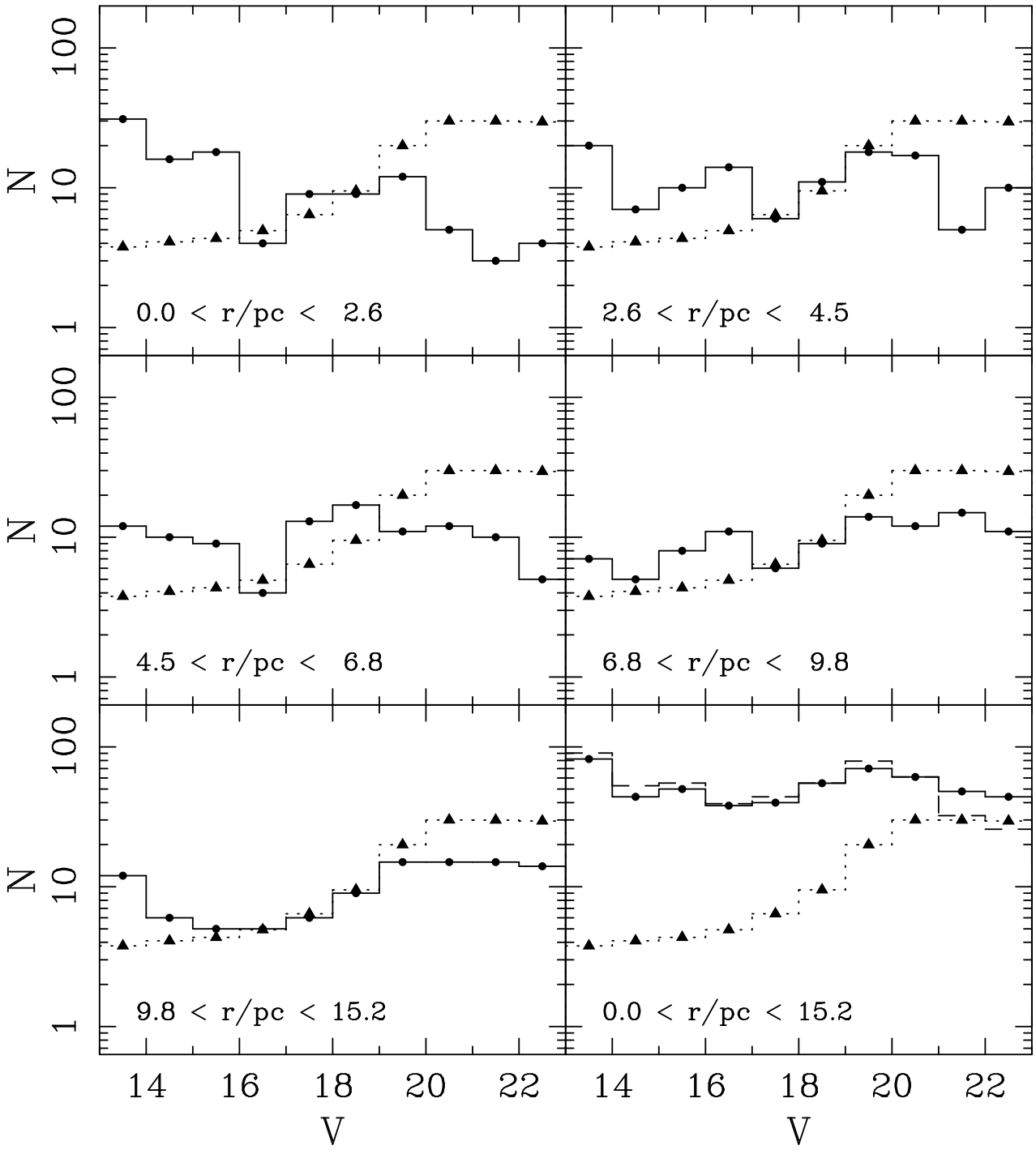

Figure 17. Luminosity function of single main-sequence stars for $13 < V < 23$ in Model 2 at 4 Gyr split into five radial regions. The regions are chosen so that there is a similar number of stars in each (about 106). The sixth panel (lower-right) shows the combined distribution. We compare this with the luminosity function for single MS stars and MS-MS binaries with $q < 0.5$ (dashed line). Also shown (dotted line with solid triangles) in each panel is the population synthesis MS luminosity function at 4 Gyr but with the number of stars in each bin reduced by a factor of 60 in order to aid comparison of the distribution slopes.

Table 1. Parameters of the starting models at time zero for simulations performed in this work (see text for details).

	Model 1	Model 2
$N_{\rm s}$	9000	12000
$N_{\rm b}$	9000	12000
$R_{\rm G}$/kpc	8.5	8.0
$v_{\rm G}$/km/s	220	220
density profile	Plummer	Plummer
binary periods	Kroupa	flatlog
$M_0/M_\odot$	14405	18687
$T_{\rm rh,0}$/Myr	300	290
$R_{\rm t}$/pc	34.4	31.8
$R_{\rm h}$/pc	4.3	3.9

Table 2. General results at 4 Gyr for simulations performed in this work.

	Model 1	Model 2
$M/M_\odot$	3175	2037
$f_{\rm b}$	0.53	0.60
$T/T_{\rm rh}$	9	13
$R_{\rm t}$/pc	20.8	15.2
$R_{\rm h}$/pc	4.9	3.8
$M_{\rm L}/M_\odot$	1987	1488
$M_{\rm L10}/M_\odot$	1730	1342
$R_{\rm h,L10}$/pc	3.0	2.7

Table 3. Stellar population results at 4 Gyr for simulations performed in this work (see text for details).

	Model 1	Model 2
$N_{\rm BS}$	1	20
$N_{\rm BS,bin}$	1	9
$N_{\rm BS}/N_{\rm MS,2to}$	0.01	0.18
$R_{\rm h,BS}$/pc	–	1.1
$N_{\rm RS}$	2	6
$N_{\rm CV}$	3	1
$f_{\rm WD}$	0.16	0.15
$R_{\rm h,WD}$/pc	0.3	0.6

Table 4. Details of the blue stragglers observed in Model 2 at 4 Gyr. Columns are the star ID number for the BS, mass of the BS, its V-band magnitude and $(B-V)$ colour (that of the BS or unresolved BS-binary), the radial position in the cluster at 4 Gyr, and the time at which the BS obtained its current mass. If the BS is in a binary the companion type is given in Column 7 followed by the companion mass, orbital period and eccentricity. The final column gives a classification of the evolution history of the BS using the following key: prim = primordial binary; A = Case A mass transfer leading to coalescence; B = Case B mass transfer; C = Case C mass transfer; coll = collision in eccentric binary; exch = exchange interaction; and pert = perturbation to orbit.

ID#	$M/M_\odot$	V	$(B-V)$	r/pc	T_0/Myr	type	$M_2/M_\odot$	P/d	e	history
3289	2.10	10.95	0.12	1.03	3613	MS	1.3	81.3	0.86	exch–coll–coll
1418	2.09	10.82	0.20	0.37	3844	giant	0.7	1.95	0.00	C–exch–B
2203	2.08	10.94	0.17	1.10	3480	MS	0.8	363	0.30	pert–coll–exch–pert
2411	1.97	11.61	0.07	0.49	3657	–	–	–	–	prim–pert–A
2565	1.89	11.44	0.22	19.38	3652	–	–	–	–	prim–pert–coll
1613	1.88	11.36	0.34	0.92	2871	MS	0.9	11749	0.27	exch–A–exch
2321	1.88	11.71	0.13	1.74	3971	MS	0.7	26.9	0.65	prim–pert–coll
2737	1.80	11.56	0.39	0.91	2549	–	–	–	–	prim–A
2855	1.74	11.84	0.28	2.11	2946	–	–	–	–	prim–A
3835	1.73	11.90	0.26	0.31	3798	MS	1.0	19498	0.69	pert–coll–exch–coll
2973	1.69	11.93	0.38	1.10	3115	–	–	–	–	prim–pert–coll
3021	1.67	12.17	0.27	2.96	3313	–	–	–	–	prim–pert–A
3157	1.63	12.04	0.56	3.08	1948	–	–	–	–	prim–A
3121	1.64	12.32	0.27	0.66	3885	MS	0.3	28184	0.72	pert–coll–exch
3207	1.61	12.27	0.34	2.44	3803	–	–	–	–	prim–A
3445	1.53	12.36	0.60	4.42	2768	MS	0.3	8511	0.58	pert–coll–exch
3523	1.51	12.77	0.35	0.75	3896	–	–	–	–	prim–A
3877	1.40	12.82	0.52	1.31	1425	–	–	–	–	prim–A
3885	1.40	12.80	0.54	1.65	1241	–	–	–	–	prim–A
1378	1.36	12.92	0.57	1.55	1957	WD	0.6	1660	0.25	prim–C–pert

Table 5. Detailed description of the formation scenario for some of the BSs listed in Table 4.

ID#	explanation
1378	This primordial binary began with an orbital period of 14454 d, an eccentricity of 0.83 and stellar masses of 1.75 and $1.21M_\odot$. After 1954 Myr the orbit began to circularize with the more massive star on the AGB. The primary filled its Roche lobe shortly afterwards when the orbit was circular with $P = 2\,203$ d. At this point the masses were 1.02 and $1.23M_\odot$ so that CE evolution was avoided and stable Case C mass-transfer began. This phase ended when the primary had shed its entire envelope to become a $0.62M_\odot$ CO WD in a circular binary of period 1 819 d with a $1.36M_\odot$ MS star companion. This was perturbed by a third star at $T = 2\,504$ Myr when 0.35 pc from the cluster centre. The period was reduced to 1 659 d and an eccentricity of 0.25 was induced.
1418	The proto-BS originated as a $1.23M_\odot$ star in a binary of period 4 466 d and eccentricity 0.7 with a $1.67M_\odot$ companion. After 2 243 Myr the initially more massive star had evolved to the AGB and wind mass loss had reduced it to $1.21M_\odot$ while tidal forces had circularized the orbit ($P = 1\,750$ d). At this point Case C mass-transfer began. This ended with a $0.64M_\odot$ CO WD and a $1.45M_\odot$ MS star in a circular orbit with $P = 1\,445$ d. At $T = 3\,243$ Myr it was involved in an exchange with a $1.35M_\odot$ star. The WD was ejected to leave a binary with $e = 0.98$ and $P = 3\,631$ d. At $T = 3\,844$ Myr the $1.35M_\odot$ star evolved off the MS, tides circularized the orbit and Case B mass-transfer started (ongoing at 4 Gyr).
1613	A primordial binary of period 47 860 d and eccentricity 0.8 containing stars of mass 1.46 and $0.3M_\odot$ became involved in a four-body interaction with another primordial binary ($P = 3\,782$ d, $e = 0.65$ and masses of 0.42 and $0.38M_\odot$) after 2 089 Myr. From this a short-period eccentric binary containing the 1.46 and $0.42M_\odot$ stars was formed ($P = 1.1$ d, $e = 0.8$). At $T = 2\,871$ Myr the binary had circularized and the $1.46M_\odot$ MS star began Case A mass transfer quickly followed by coalescence. The $1.88M_\odot$ single BS became involved in a three-body hierarchy at $T = 2\,932$ Myr with a wide primordial binary (0.86 and $0.81M_\odot$) in the cluster core. Eventually the least massive star was ejected from the system.
2203	The proto-BS began life as a $1.23M_\odot$ star with a $0.85M_\odot$ companion in a primordial binary of period 363 d and an eccentricity of 0.3. After 3 479 Myr a binary–binary encounter left this binary as the inner component of a four-body system with stars of mass 0.83 and $0.58M_\odot$. The eccentricity of the inner binary was driven up to 0.99 so that the stars collided and formed the $2.08M_\odot$ BS. The $0.58M_\odot$ star escaped the system and the BS remained bound to the $0.83M_\odot$ MS star ($P = 372$ d, $e = 0.84$). A subsequent interaction reduced the period to 363 d and the eccentricity to 0.3.
2321	This primordial binary was originally comprised of 1.29 and $0.73M_\odot$ stars in a circular orbit with a period of 31 d. At $T = 3\,360$ Myr while in the core of the cluster this binary had a close encounter with another primordial binary to form a quadruplet system. An eccentricity of 0.15 had been induced into the binary at this point. At $T = 3\,971$ Myr the $1.29M_\odot$ star collided with a $0.59M_\odot$ MS star – the relative eccentricity of these two stars had reached 0.99 – to form the $1.88M_\odot$ BS. The BS remained bound to its original companion and the fourth star ($0.41M_\odot$) was ejected.
2411	This began in a circular primordial binary with 1 d period and component masses 1.29 and $0.68M_\odot$. Case A mass-transfer was expected to start at 4 320 Myr but perturbation at 3 100 Myr while binary was in the core hardened the orbit and mass-transfer began at 3 260 Myr. Angular momentum loss from the binary lead to coalescence of the stars at 3 657 Myr.
2565	This started in a primordial binary with 3 236 d period and eccentricity of 0.32. The orbit was wide enough that interaction between the 0.95 and $0.94M_\odot$ stars was not expected. Perturbation to the orbit while the binary was 1.0 pc from the cluster centre increased the eccentricity to 0.99. The orbit became chaotic and the stars collided and merged at $T = 3\,652$ Myr.
2973	This is similar to #2565. Interaction was not expected in a wide primordial binary with $P = 4\,075$ d and $e = 0.59$. A perturbation pumped the eccentricity to 0.99 so that the 0.89 and $0.80M_\odot$ MS stars collided and merged at $T = 3\,115$ Myr.
3021	This originated in a circular primordial binary with $P = 0.7$ d and component masses 1.01 and $0.66M_\odot$ that was expected to begin Case A mass-transfer after 1 413 Myr. Prior to this, at $T = 1\,010$ Myr, the binary was involved in a short-lived exchange encounter. The primordial binary emerged intact but the period had increased enough to delay the onset of mass-transfer until $T = 2\,900$ Myr. The stars merged at $T = 3\,313$ Myr.
3121	This was a primordial binary composed of 1.09 and $0.54M_\odot$ stars with a period of 562 d and an eccentricity of 0.31 which became part of a sextuplet after 3 762 Myr. The eccentricity of the binary was increased by perturbations from the other members until at $T = 3\,885$ Myr the orbit became chaotic, the eccentricity reached 0.99 and the two stars collided. The resulting $1.64M_\odot$ BS remained bound to a $0.33M_\odot$ member of the sextuplet to give the binary observed at 4 Gyr.
3289	Two short-period circular primordial binaries ($P = 1.3$ d, $M_1 = 0.82M_\odot$, $M_2 = 0.76M_\odot$ and $P = 4.2$ d, $M_1 = 1.25M_\odot$, $M_2 = 0.51M_\odot$) became embroiled in a four-body system after 3 611 Myr. The 0.82 and $0.51M_\odot$ stars formed an inner binary and collided after the eccentricity was pumped up to unity. The collision product then collided with the $0.76M_\odot$ star to form a $2.09M_\odot$ BS. The BS remained bound to the $M_1 = 1.25M_\odot$ MS star in an eccentric orbit with $P = 81$ d.
3445	The proto-BS originated as a $0.78M_\odot$ star in a 2.9 d circular orbit with a $0.75M_\odot$ companion. No interaction between the stars was expected in this short-period primordial binary. After 2 768 Myr the binary formed a triple system with a $0.25M_\odot$ star. The close presence of the third star induced an eccentricity of 0.84 into the binary orbit so that the stars came into contact and merged. The $1.53M_\odot$ merged star remained bound to the $0.25M_\odot$ star.
3835	A primordial binary consisting of 0.82 and $0.60M_\odot$ stars in a 1.8 d circular orbit became involved in a four-body system with another binary (formed earlier from an exchange) at $T = 3\,797$ Myr. The stars in the primordial binary collided and merged and this new star then collided with a $0.31M_\odot$ star to form a $1.73M_\odot$ BS. The BS remained bound to the fourth member of the system, a $1.04M_\odot$ MS star, in a long-period eccentric orbit.

Table 6. Details of the RS CVn binaries observed in Model 2 at 4 Gyr. The first column gives the star ID number for the subgiant star and this is followed by the mass of the subgiant. Column 3 gives the mass of the MS star companion. The V-band magnitude and $(B-V)$ colour of the unresolved binary are then given. The sixth column gives the radial position in the cluster of the binary at 4 Gyr. The orbital period and eccentricity are given in Columns 7 and 8, respectively. Some remarks on each binary are provided in the final column.

ID#	$M_1/M_\odot$	$M_2/M_\odot$	V	$(B-V)$	r/pc	P/d	e	remarks
1568	1.33	0.95	12.50	0.60	0.27	1.6	0.0	exchange
1799	1.36	1.08	12.30	0.88	4.91	5.0	0.0	primordial
2335	1.33	0.68	12.69	0.68	0.28	3.0	0.0	primordial
2383	1.37	0.62	10.49	1.17	1.32	19.8	0.0	primordial
2633	0.63	1.19	13.82	0.64	1.11	0.4	0.0	primordial; semi-detached
2873	1.33	0.40	12.05	0.63	8.46	6.2	0.0	primordial